TUNING FORKS AS A GENERATOR OF QUANTUM TURBULENCE IN SUPERFLUID HELIUM

V.B. Efimov,
Institute of Solid State Physics RAS, Chernogolovka, 142432,
Moscow distr., Russia

VIII-th International Conference,
"SOLITONS, COLLAPSES and TURBULENCE
In honor of Evgenii Kuznetsov's 70th birthday

22 May 2017

Report outline

- Quantum turbulence in superfluid helium
- Vortex generation by vibrating bodies
- Tuning forks, electro-mechanical coefficient
- Tuning fork as a turbulence generator
- Tuning fork as a vortex detector
- Two regimes of vortex generation
- New type of tuning forks

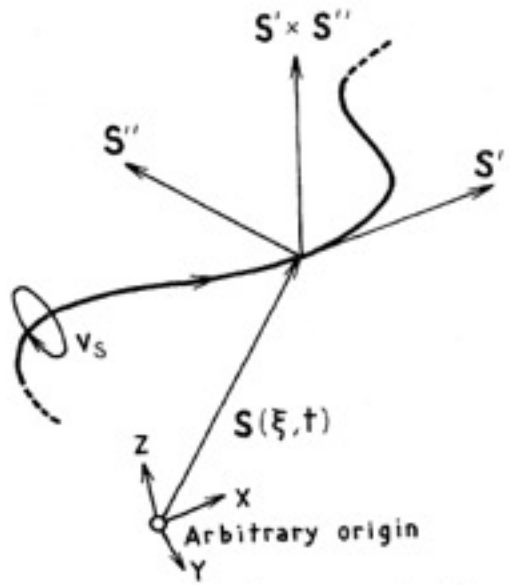

FIG. 1. Space curve representing a vortex line with its position described as $\mathbf{S}(\tilde{\xi},t)$, when ξ is arclength. $\mathbf{S}'=d\mathbf{S}/d\xi$ is a unit vector along the vortex line; $\mathbf{S}''=d^2\mathbf{S}/d\xi^2$ is the local curvature vector (whose magnitude is $1/R$); and $\mathbf{S}'\times\mathbf{S}''$ is binormal, which also has the magnitude $1/R$ (Donnelly, 1991, Fig. 1.14).

A motion of superfluid component could be written as

$$\omega(\mathbf{r})=\mathrm{rot}\mathbf{v}_s=\kappa\int d\mathbf{S}\delta(\mathbf{r}-\mathbf{S}(\xi,t))$$

where the integration is along the line singularity $S(\xi, t)$.
A single infinite straight line induces a velocity field, described in cylindrical coordinates by

$$\mathbf{v}_s=\left(0,\frac{\kappa}{2\pi r},0\right)$$

Having only an azimuthal component which increases rapidly on approaching the vortex axis. In particular, at r≤3Å, the velocity v_S becomes greater than the velocity of roton generation, i.e., Landau's velocity.

Vortexes in superfluid helium

Quantization of vortex lines, core radius a_0 and intervortex distance ℓ

$\oint \boldsymbol{v}_S \cdot d\boldsymbol{r} = n\,\kappa$, where $\kappa = \dfrac{2\pi\hbar}{M}$ is the circulation quant.

$M = 4$ for ^{4}He and $M = 6$ for a pair of ^{3}He atoms.

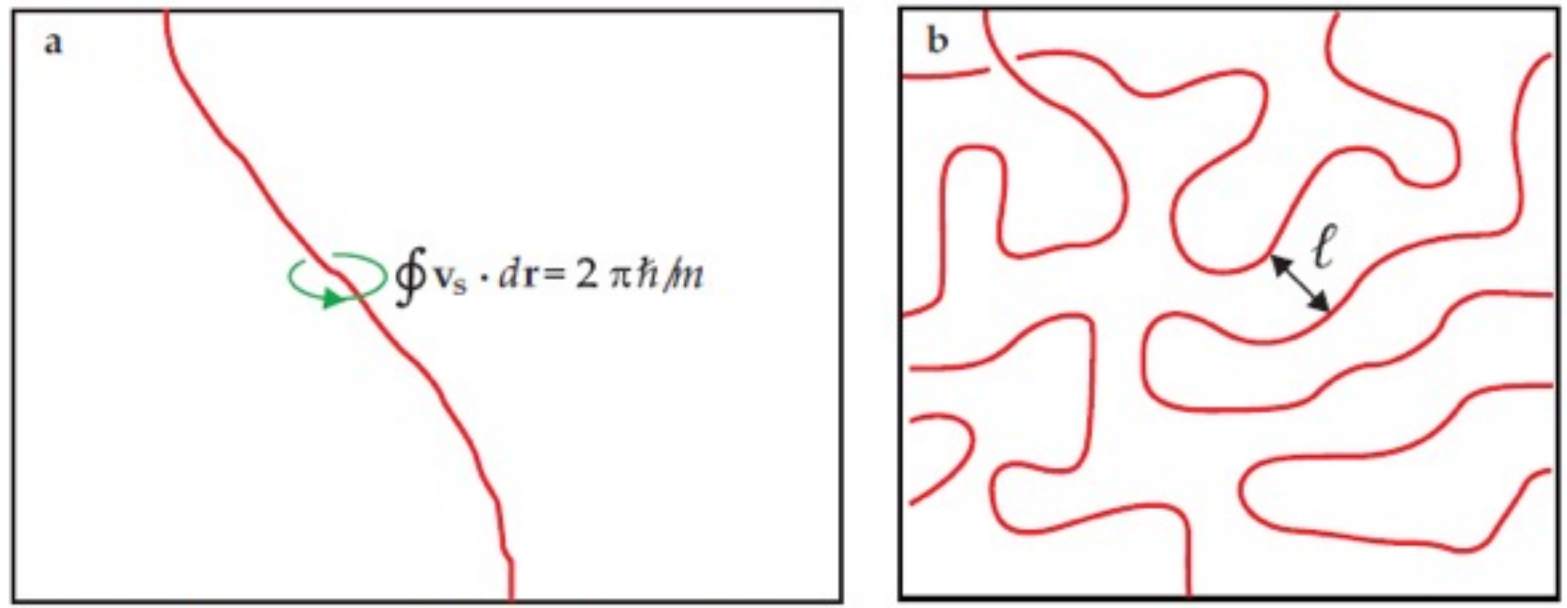

- ℓ is the mean intervortex distance,
- Vortex core radius $a_0 \simeq 1$ Å for ^{4}He & $a_0 \simeq 800$ Å at low p.

for ^{3}He

Classical turbulence – measures of its intensity

Reynolds number

$$\mathrm{Re} = \frac{UL}{\nu}$$

For isothermal flows

T(P)

ν (cm²/s)=10⁻² St

kinematic viscosity

air	**20 C**	**0,15**
water	**20 C**	**1,004x10⁻²**
ethanol	**20 C**	**0.022**
mercury	**20 C**	**1,2x10⁻³**
Helium I	**2,25 K (VP)**	**1,96x10⁻⁴**
Helium II	**1,8 K (VP)**	**9,01x10⁻⁵**
He-gas	**5,5 K (2,8 bar)**	**3,21x10⁻⁴**

•He II and 3He B – so far the only two media where quantum turbulence has been systematically studied under controlled laboratory conditions

Counterflow turbulence phenomenology (Vinen 1957)

Vortex ring

$$\mathbf{v}_t = \frac{\kappa}{4\pi b}\left(\ln\frac{8b}{a} - \frac{1}{4}\right) \cong \frac{\kappa}{b}$$

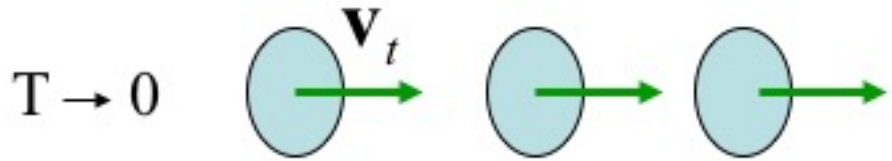

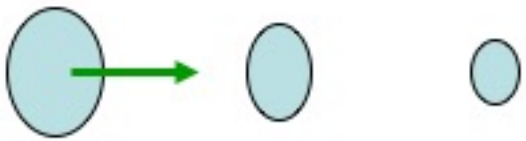

In counterflow, though, if $|\mathbf{v}_t| < |\mathbf{v}_n - \mathbf{v}_s| = V_{CF}$ rings with $b > b_c$ expand

Dimensional analysis and analogy with classical fluid dynamics leads to the Vinen equation:

$$\frac{dL}{dt} = \chi_1 \frac{B}{2}\frac{\rho_n}{\rho} V_{CF} L^{3/2} - \chi_2 \frac{\hbar}{m_4} L^2 + (g(V_{CF}))$$

production **decay**

Reproduced by Schwarz (1988) – computer simulations
Local induction approximation
Importance of reconnections

^{4}He

T

normal liquid He I

Classical Navier-Stokes fluid of
extremely low kinematic viscosity

2

Superfluid transition at Tc=2.17 K

He II – **a "mixture" of two fluids**

normal fluid of extremely low kinematic viscosity

+

Inviscid superfluid

3

Circulation is quantized

$$\kappa = \frac{2\pi \mathrm{h}}{m_4} \approx 10^{-3}[cm^2/s]$$

T → 0 limit

1

0

Pure superfluid

Maurer, Tabeling,
Europhysics Lett. 43 (1998) 29
Flow between counterrotating discs

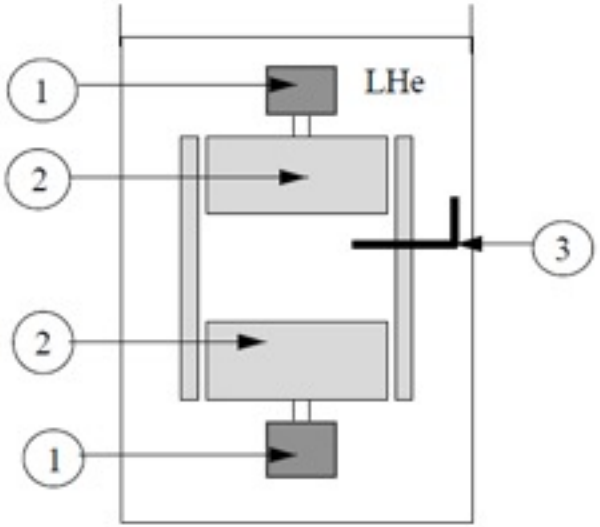

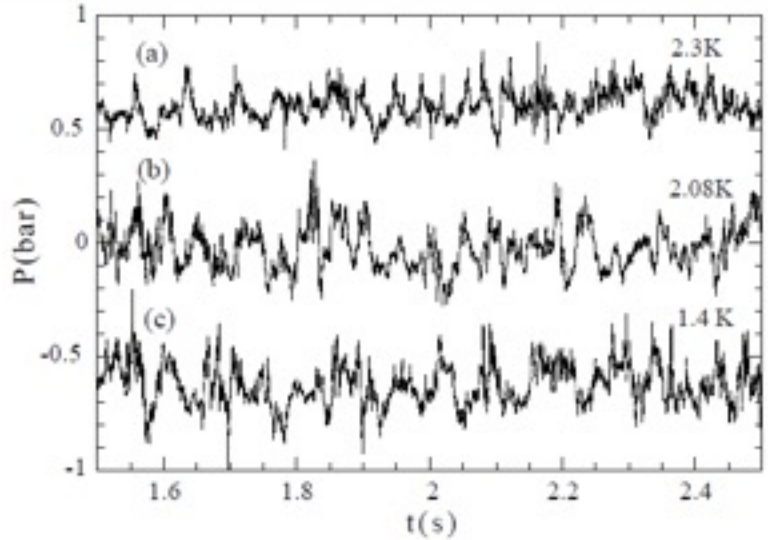

Energy spectra obtained in the same conditions:
U=80cm/s; Re=2x10^6 a-2.3K; b-2.08K; c-1.4 K
The spectra have bee shifted vertically so as to make their representation clear.

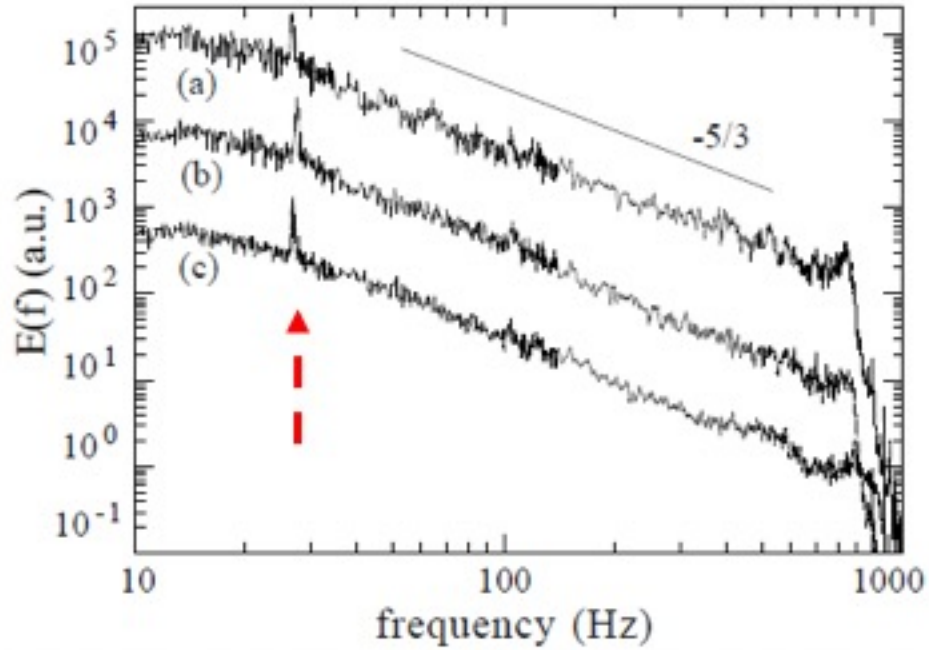

Oscillating objects used in experiments in He II and in ^{3}He

Discs and piles of discs

Hollis-Hallett

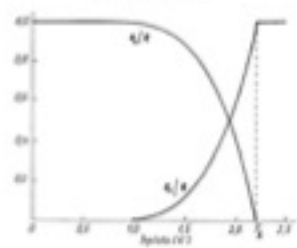

Andronikashvili

U-tubes

Donnelly

Penrose

Torsional oscillators

Many authors – vibrating wire viscometers

Vinen

Morishita, Kuroda, Sawada, Satoh, JLTP 76, 387 (1989)

Lancaster – Pickett's group, Osaka – Yano et al., Kosice Skyba et al., Moscow Dmitriev et al., Helsinki- YKI group..., Grenoble Bunkov et al., ...

Wires He II and 3He

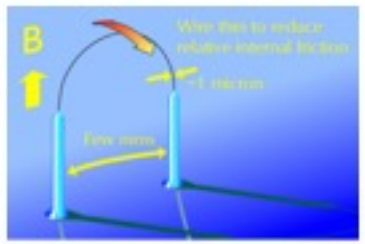

Spheres He II (3He?)

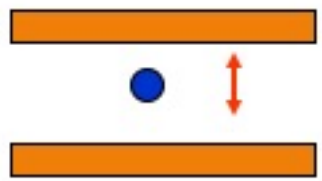

Schoepe et al

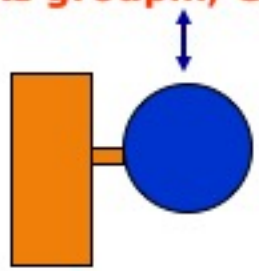

Luzuriaga

Hollis-Hallett

Lancaster – P. McClintock's group

Grids He II and 3He

Lancaster – G. Pickett's group

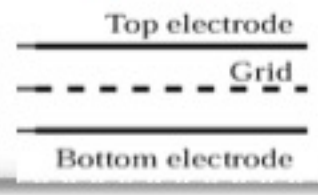

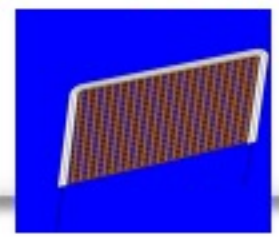

Typical characteristics of commercially available forks

Room temperature
closed fork

frequency 2^{15} Hz = 32764 Hz
linewidth around 0.5 Hz

Bare fork

frequency down by 7-10 Hz
linewidth around 5-6 Hz

Ground off can

linewidth around 3 Hz

Fork in vacuum: LN2 32722 Hz linewidth 0.2 Hz
LHe 32710 Hz linewidth 0.06 Hz
Q about 500 000

Fork in cryofluids: He I SVP 4.2 K 31600 - 31700 H
linewidth 12-13 Hz
He II SVP 1.3 K linewidth 1.2 Hz

Response to about 8 orders of magnitude of the ac drive (up to 130 V rms) fork rms velocity reaches up to 10 m/s

Thermal cycling is not a serious issue for most applications

Quartz tuning forks –

- Commercially produced piezoelectric oscillators, used as frequency standards in watches (2^{15} Hz = 32 768 Hz at room temperature)
- New addition to a family of oscillating objects, a probe to investigate physical properties of cryogenic fluids, especially gaseous He, He I, He II and ^{3}He-B
- Cheap, robust, widely available, easy to install and use (2 wires only), very sensitive
- No magnetic field needed, to which they are very insensitive

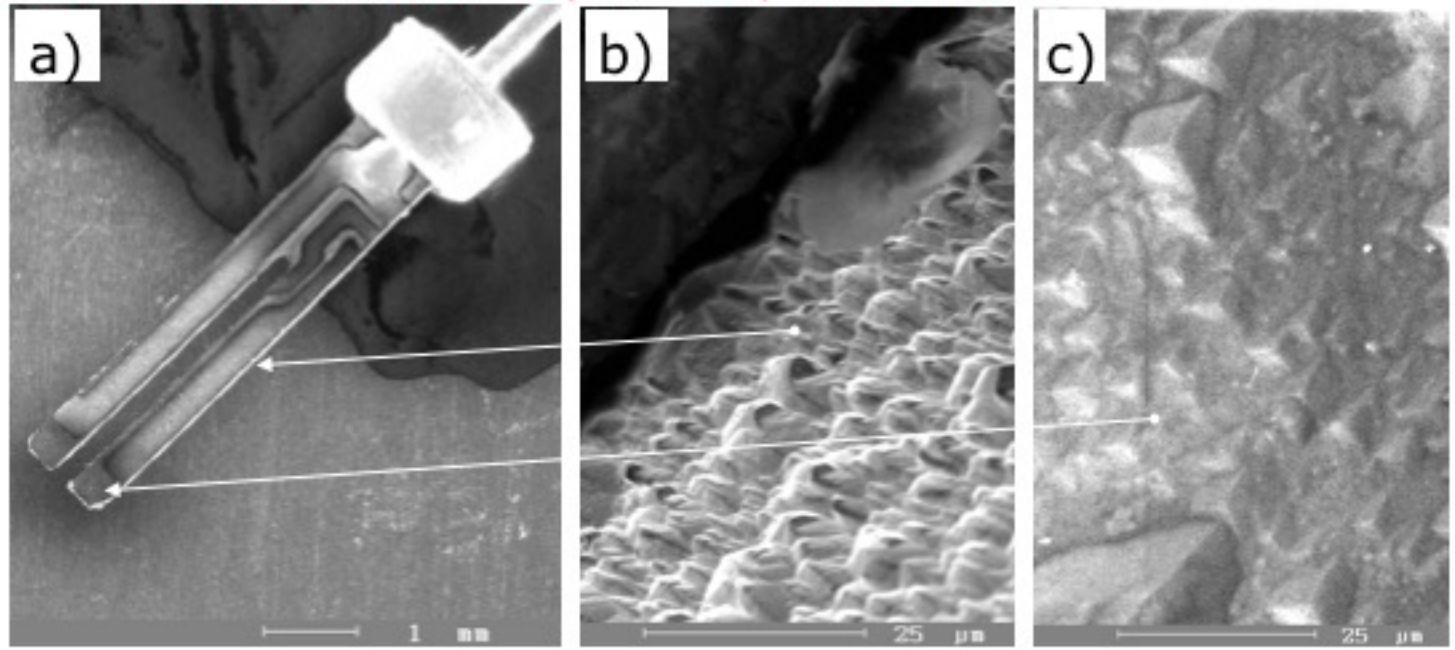

An electron micrograph of the quartz tuning fork (a) and details of its side (b) and top (c) quartz surface.

Quartz Tuning Fork: Thermometer, Pressure- and Viscometer for Helium Liquids, R. Blaauwgeers, M. Blazkova, M. Clovecko et al, *JLTP, 146, 5/6, 537 (2007)*

- **Mechanical properties**

$$\frac{d^2x}{dt^2}+\gamma\frac{dx}{dt}+\frac{k}{m}x=\frac{F}{m}$$

- Resonance frequency

$$\omega_0=\sqrt{\frac{k}{m}}$$

- Quality $Q=\frac{\omega_0}{\gamma}$, where width of resonance curve $\Delta\omega=\gamma$
- Effective mass of prong

$$m_{\mathrm{vac}}=0.24267\,\rho_{\mathrm{q}}\,\mathcal{L}\,\mathcal{W}\,\mathcal{T}$$

- **Electrical properties**
- Fork response $U=U_0\cos(\omega t)$ $I(t)=a\frac{dx(t)}{dt}$
- The mechanical oscillator with the equivalent electrical RLC series resonance circuit. The corresponding differential equation for the current is

$$\frac{d^2I}{dt^2}+\frac{R}{L}\frac{dI}{dt}+\frac{I}{LC}=\frac{1}{L}\frac{dU}{dt}$$ =>

$$F_0=(a/2)\,U_0,\quad R=2m\gamma/a^2,\quad L=2m/a^2,\quad C=a^2/(2k).$$

$\omega_0^2=1/(LC),\ \gamma=R/L,$ and $1/L=(F_0/U_0)\,a/m$

$$a=\sqrt{\frac{2m\,\Delta\omega}{R}}$$

Electro-mechanical calibration

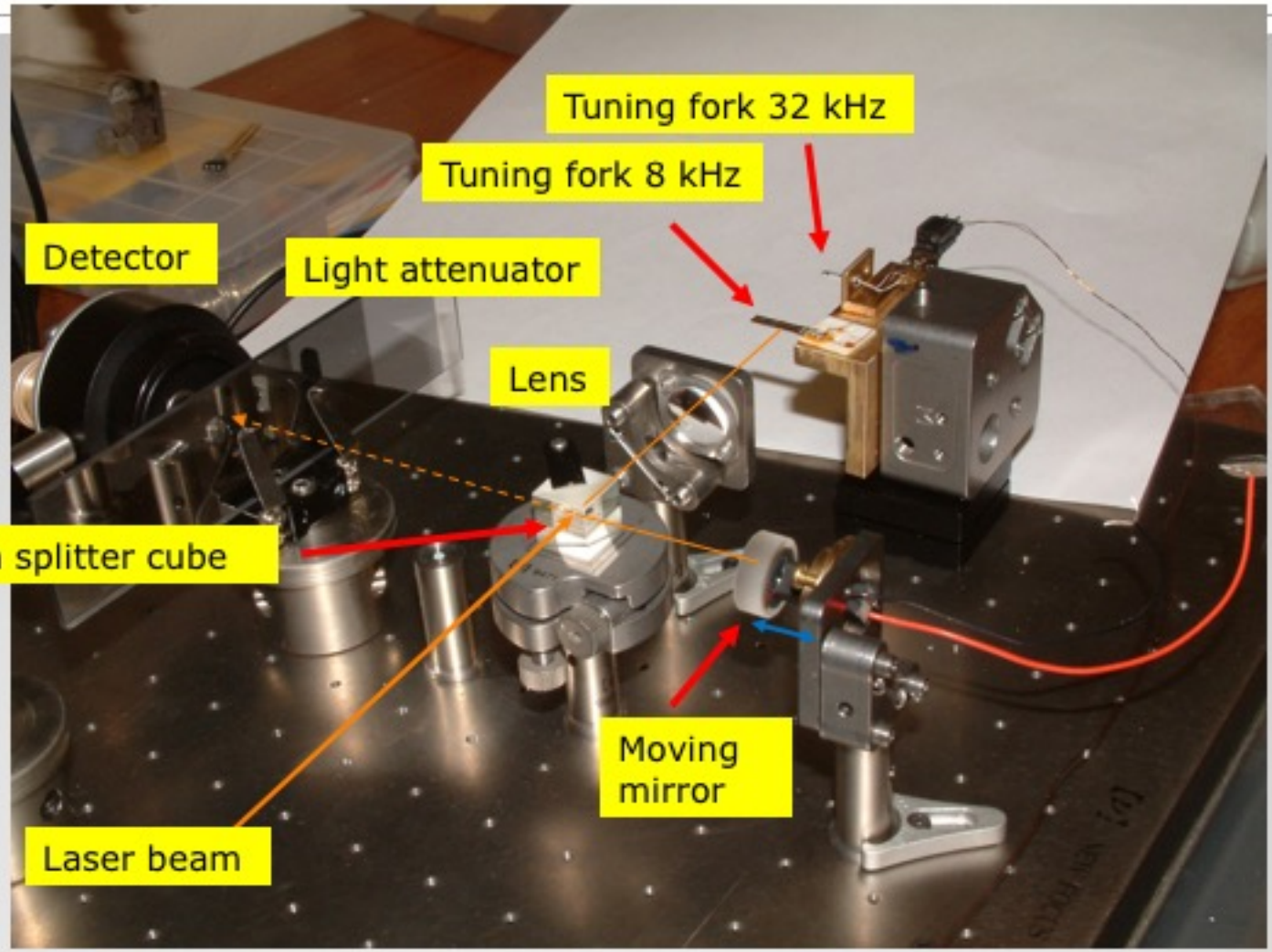

Michelson interferometer scheme for measurement of amplitude of fork vibration

Absolute prong's velocity (T_{room}, air)

Bending vibration f_C=75,64 kHz
V_{drive}=800 mV_{PP}; f = 76,228 kHz, Δf=17 Hz;
sensitivity of Doppler analyzer (DA) 100 mm/s/V
signal of DA = 4.8 V, velocity of vibration v_P=48 cm/s
No changing in DA signal at scanning perpendicular to prong width. Laser point was near the end of the fork's prong (v_{max} ~1.2* v_P)

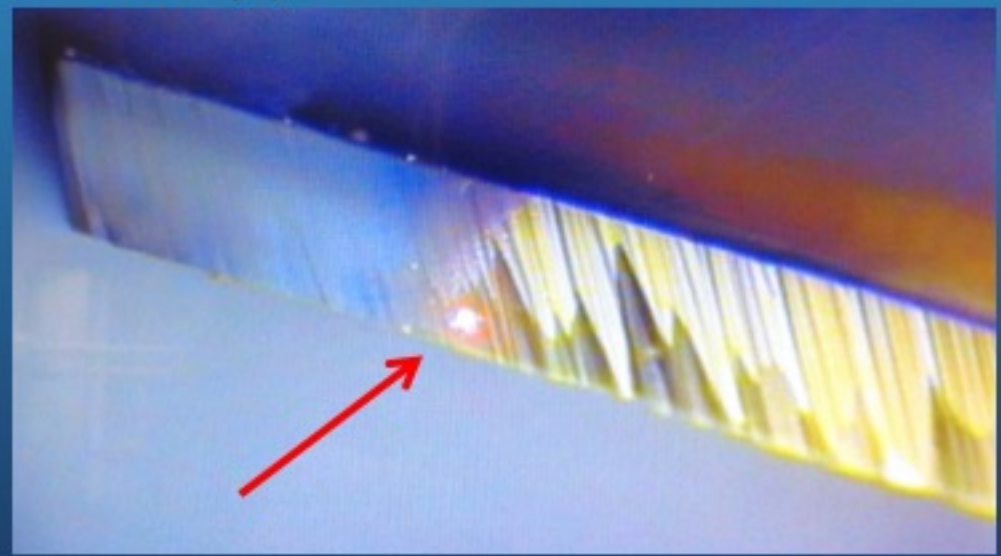

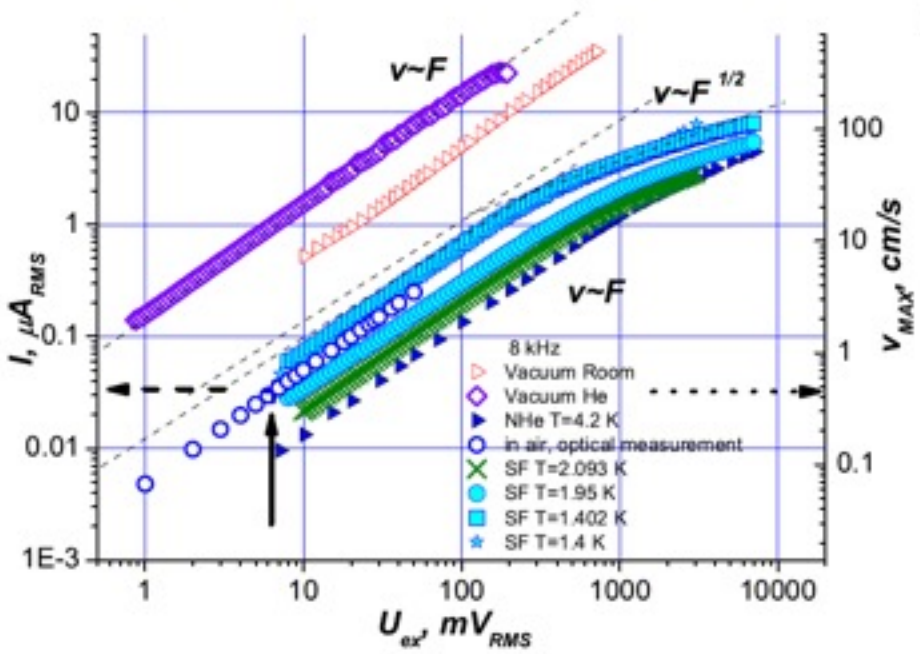

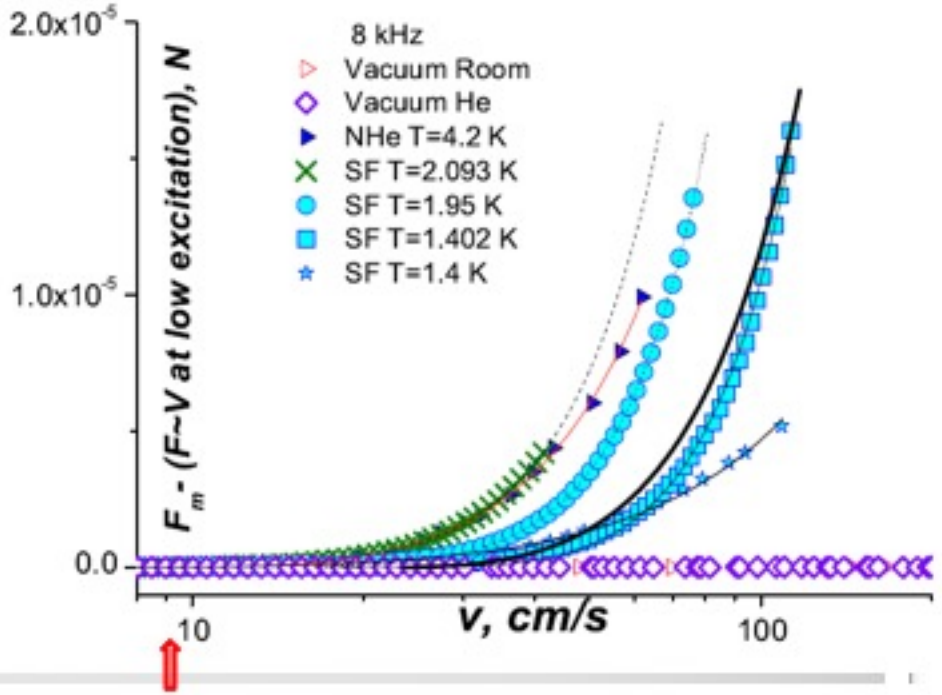

At low excitation the fork response and corresponding velocity are proportional to the driving force. Higher excitation leads to the appearance of some additional mechanism of energy dissipation and to a deviation of the fork response (and its velocity) from linear dependence. Note that such deviations were not seen in vacuum (left graphic); they are usually attributed to the transition to turbulence above a critical velocity.

We estimated the deviation of the applied force (and counteracting fluid forces) by subtracting off the extrapolated the linear dependence at low excitation.

$F_{add} = F(v) - C \times v$

The results are shown in right graphic. The fluid friction force increases very rapidly after the critical velocity v_c is attained. We fitted the deviation by power law $F_{add} = C_2 \times (v - v_c)^N$ at different temperatures.

Low temperature behaviour of 8kHz fork

Generation of the quantum turbulence by tuning fork

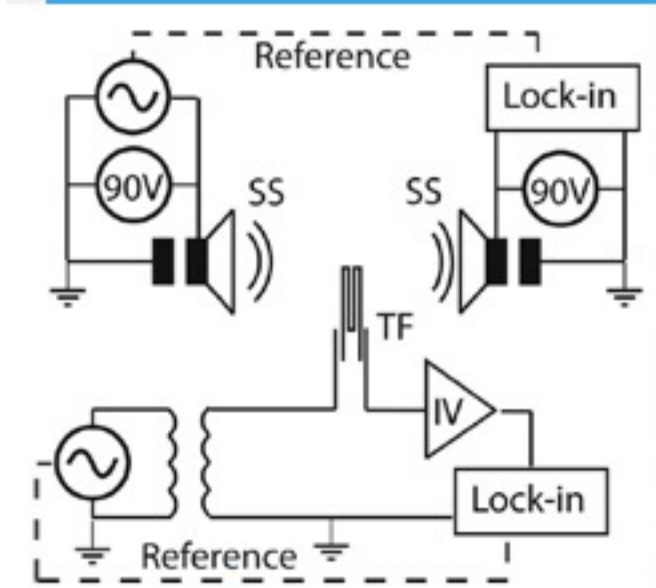

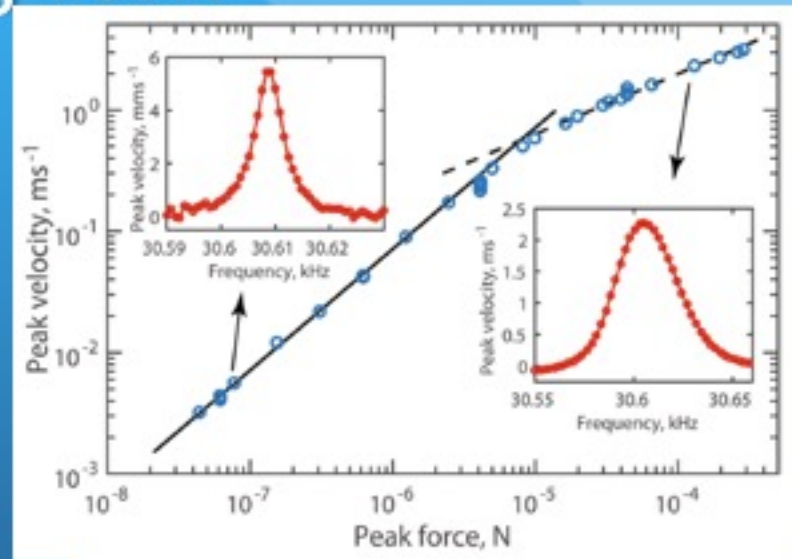

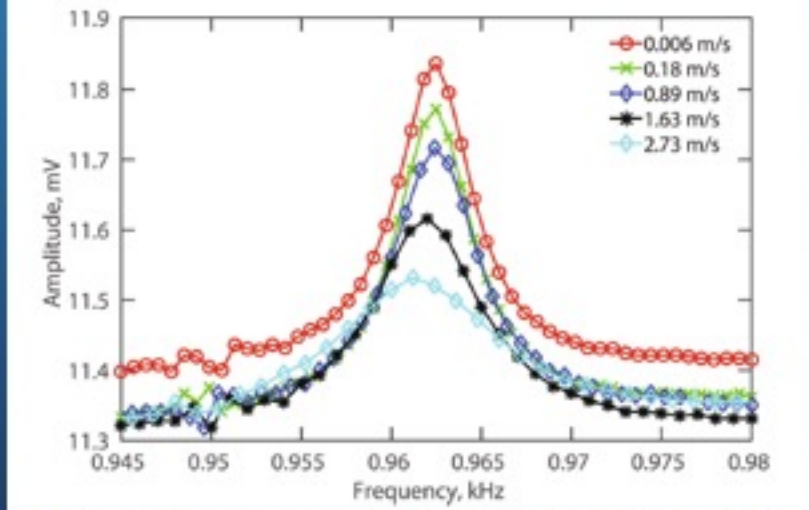

Fig. 3 Second sound frequency sweeps of the 5th second sound mode at various tuning fork velocities. [illegible] the resonant frequency caused by [illegible] and velocity due to the competition between a [illegible] and [illegible] (Color figure online)

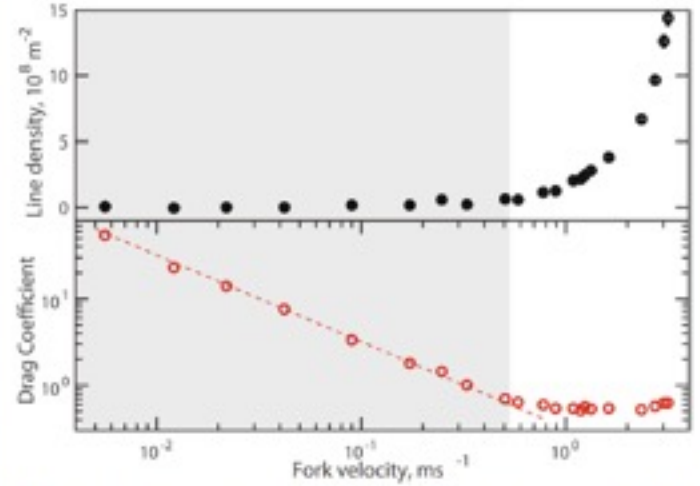

Fig. 4 *Top Vortex line* density inferred from the second sound attenuation as a function of tuning fork velocity. *Bottom* drag coefficient experienced by the tuning fork versus tuning fork velocity. The *dashed line* is a guide for the eye and the *shaded area* highlights the laminar regime. For details, see text (Color figure online)

M.J.Jackson et al., JLTP 183, 208 (2016)

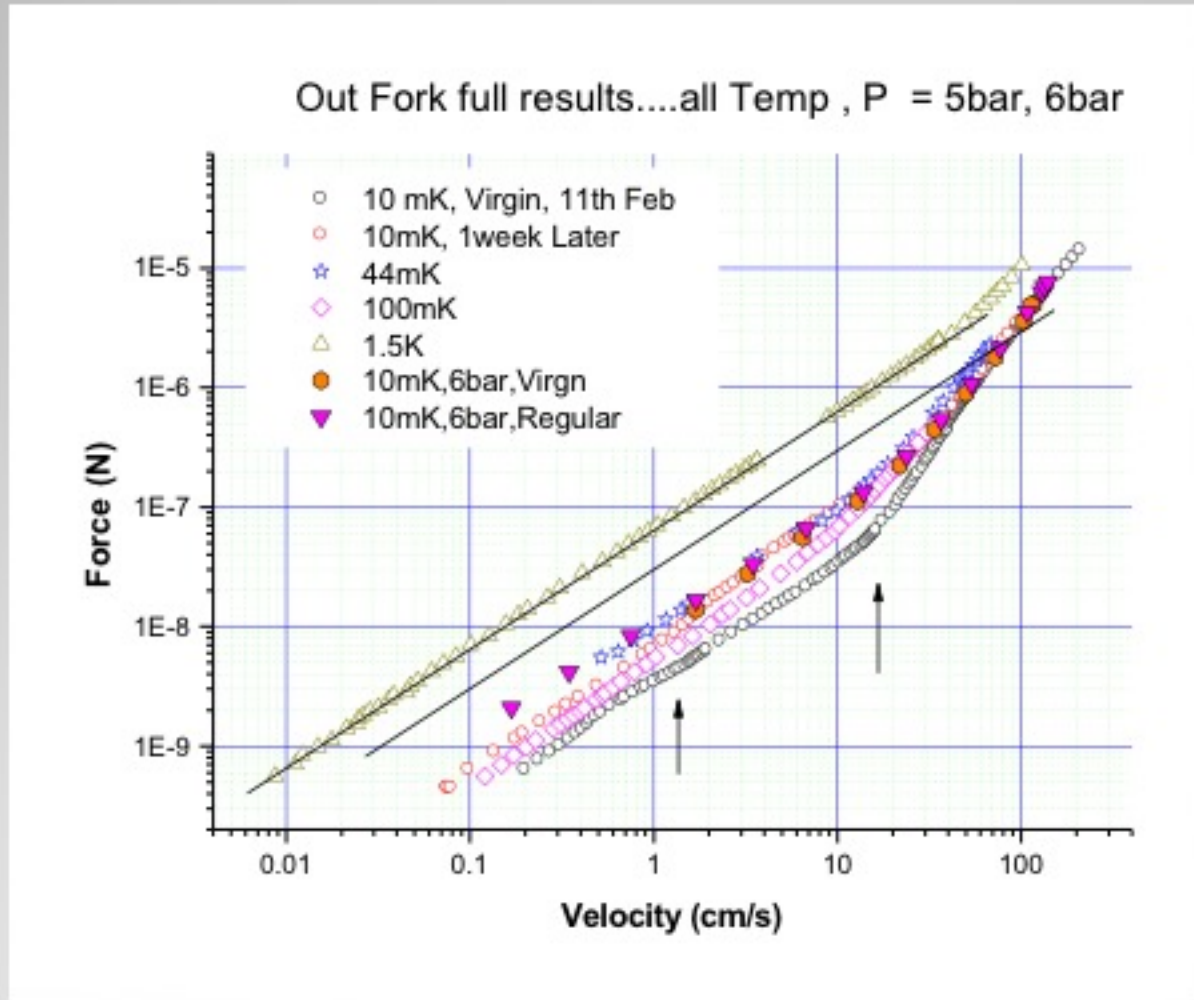

Temperature behaviour of fork response

Current-voltage characterictic (T > 1 K).

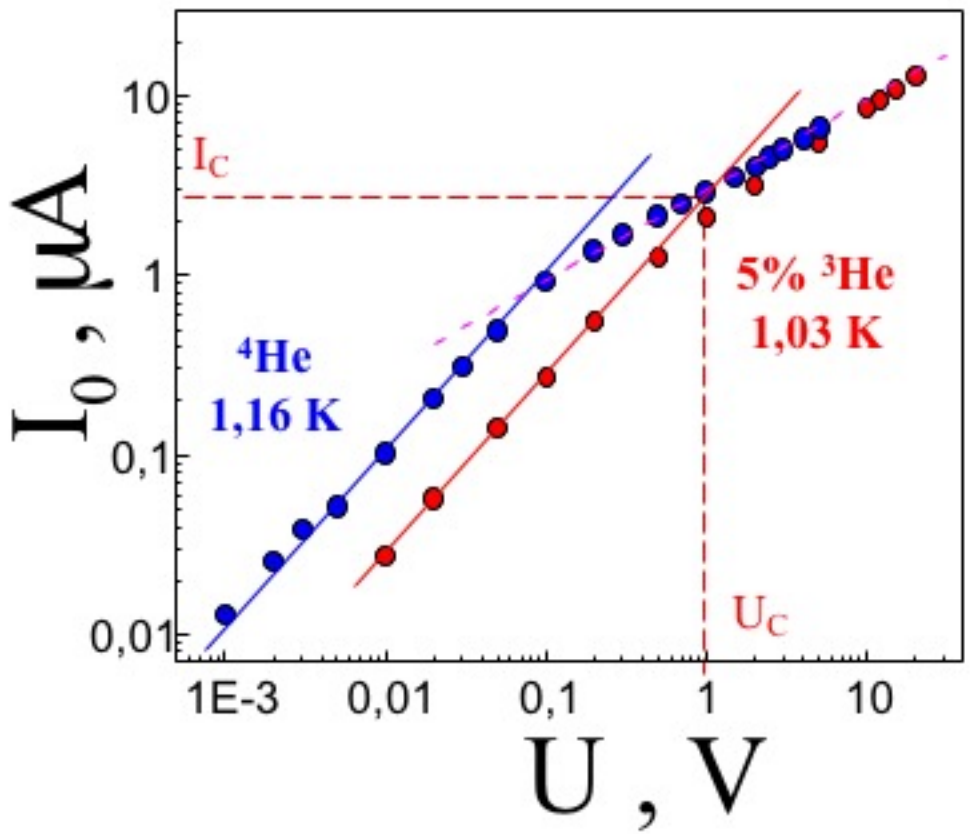

At low U: $U \sim I_0$

laminar regime

(solid lines)

At high U: $U \sim I_0^2$

turbulence

(dashed line)

The laminar flow is more stable in the ^{3}He-^{4}He mixture than that in pure ^{4}He

Vortex propagation in superfluid helium

The have studied the vortex motion through superfluid helium. One of the standard 32 kHz fork was used as a generator of vorticity, another one was used as a detector of vortexes. The scheme of experiment is shown on Fig.3.

The resonance frequencies of forks differ on 0.5 kHz.

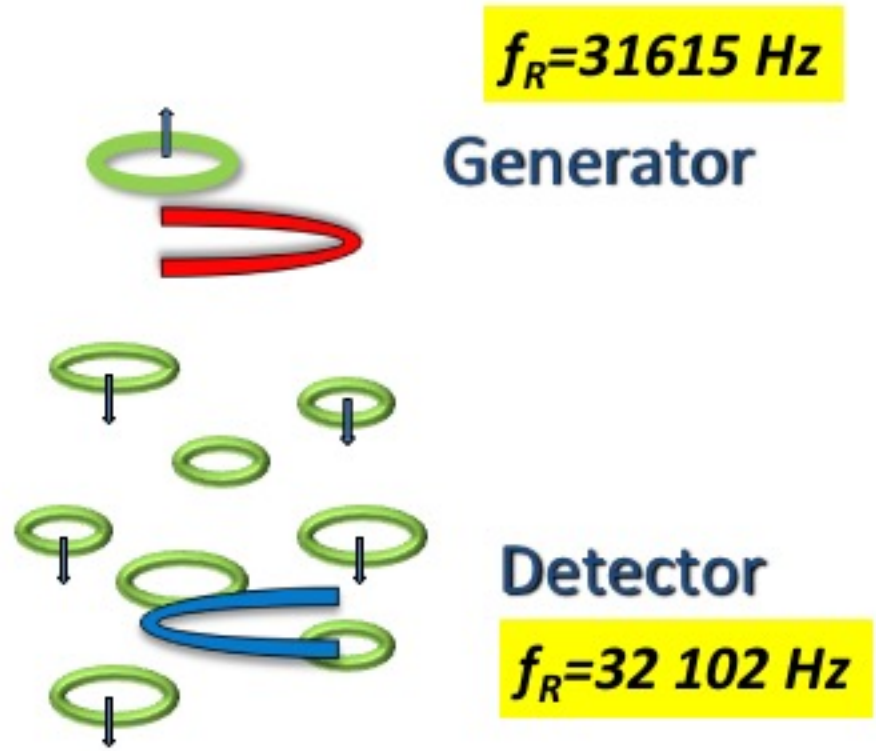

Fig 3. Scheme of experiments of vortex propagation. One of the forks was used as a generator with different excitation, another – as a detector with low oscillation. We mutual changed a function generator-detector for both forks.

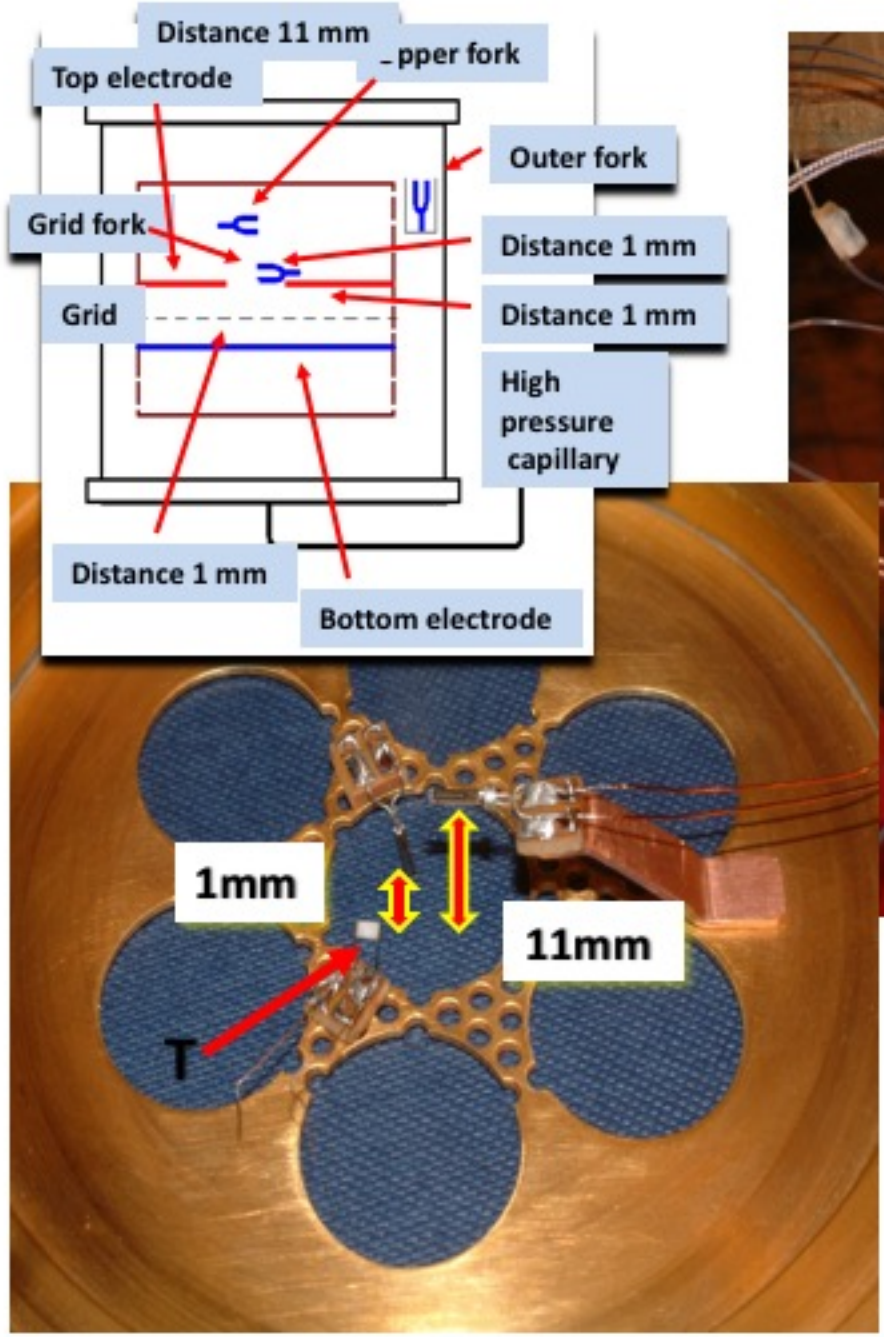
Distance 11 mm
Top electrode
Upper fork
Outer fork
Grid fork
Distance 1 mm
Grid
Distance 1 mm
High pressure capillary
Distance 1 mm
Bottom electrode
1mm
11mm
T

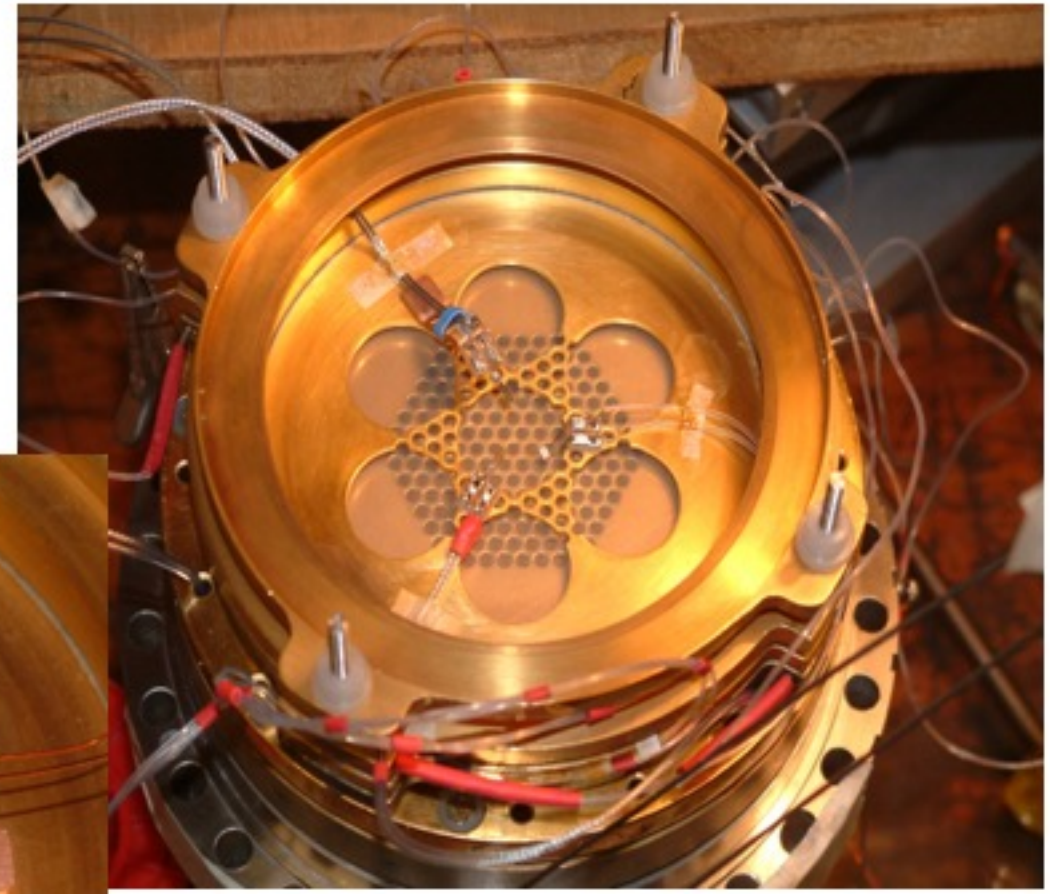

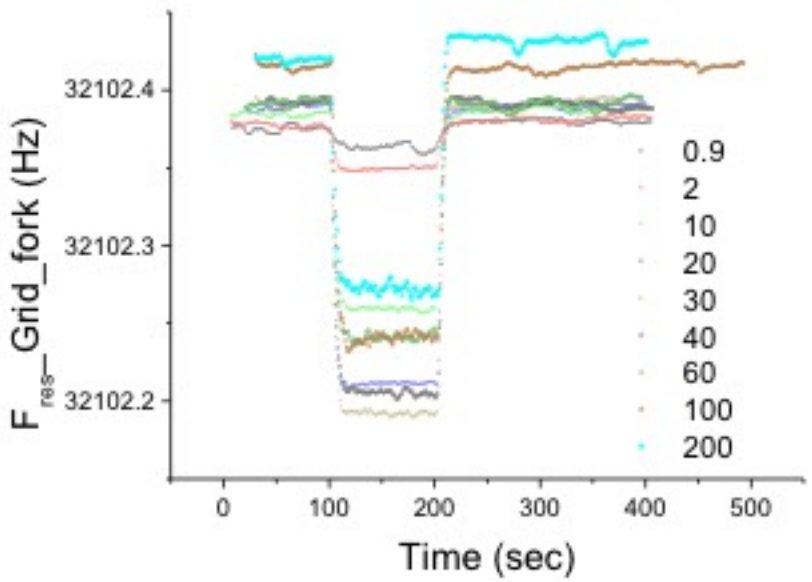

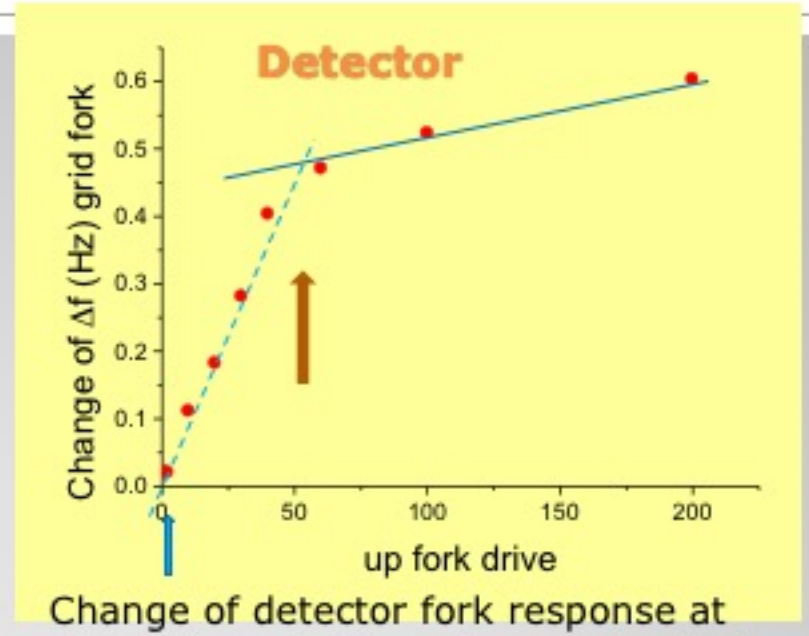

Change of detector fork response at different excitations of generator fork

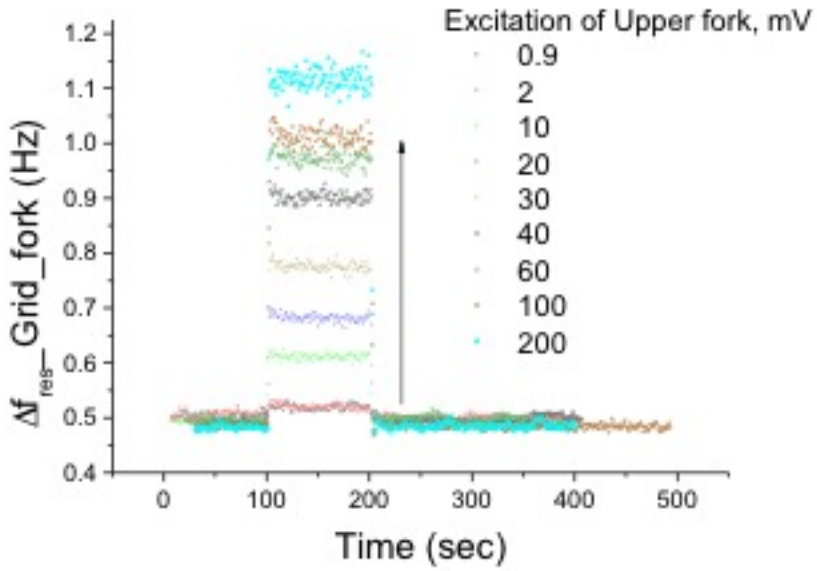

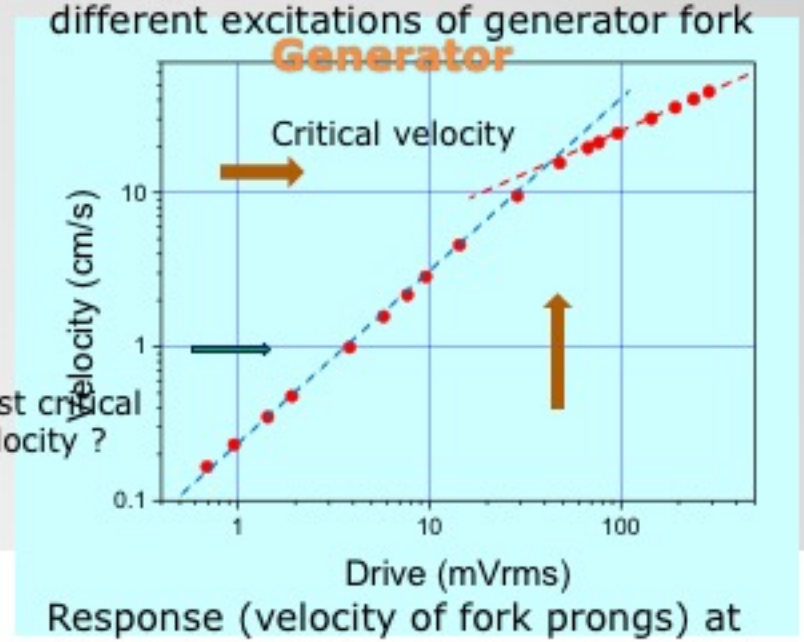

First critical velocity ?

Response (velocity of fork prongs) at different excitations for generator fork.

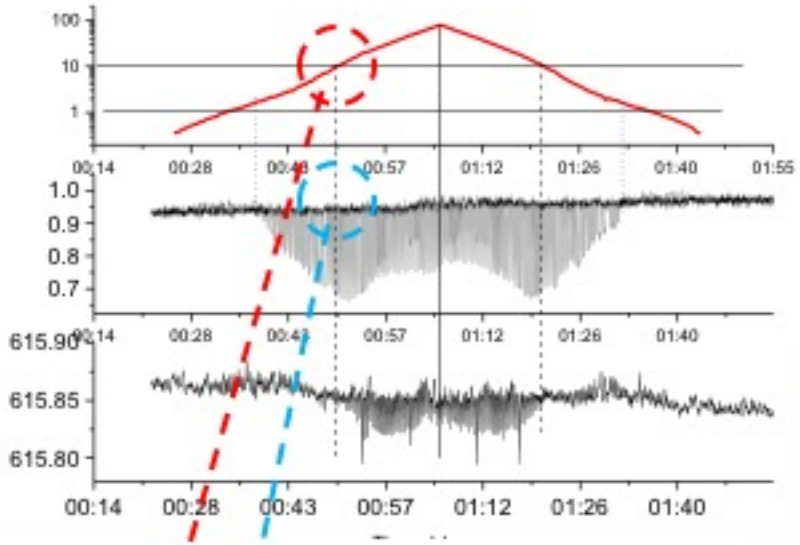

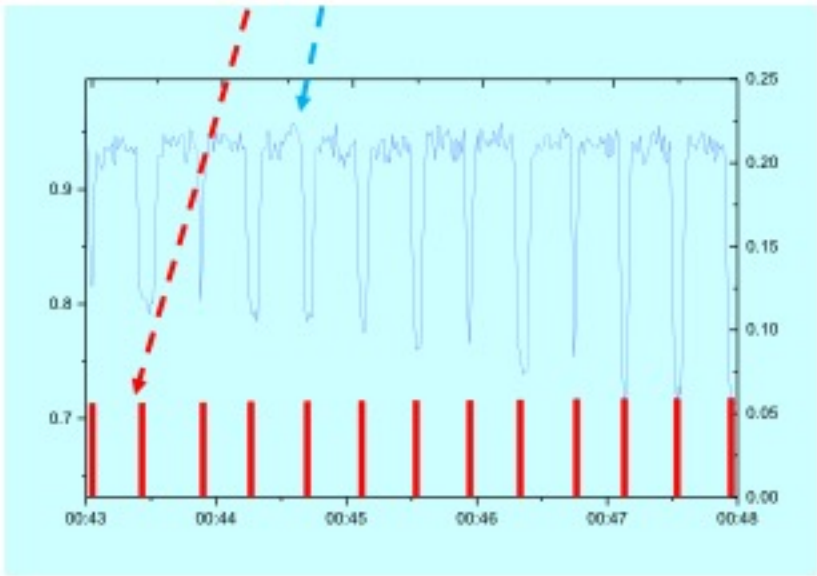

Fig 6: Time dependence of detector response at changing of generator excitation.

Excitation was done by telegraph code – signal with amplitude U_G - 2 s and waiting time with zero excitation 20 s.

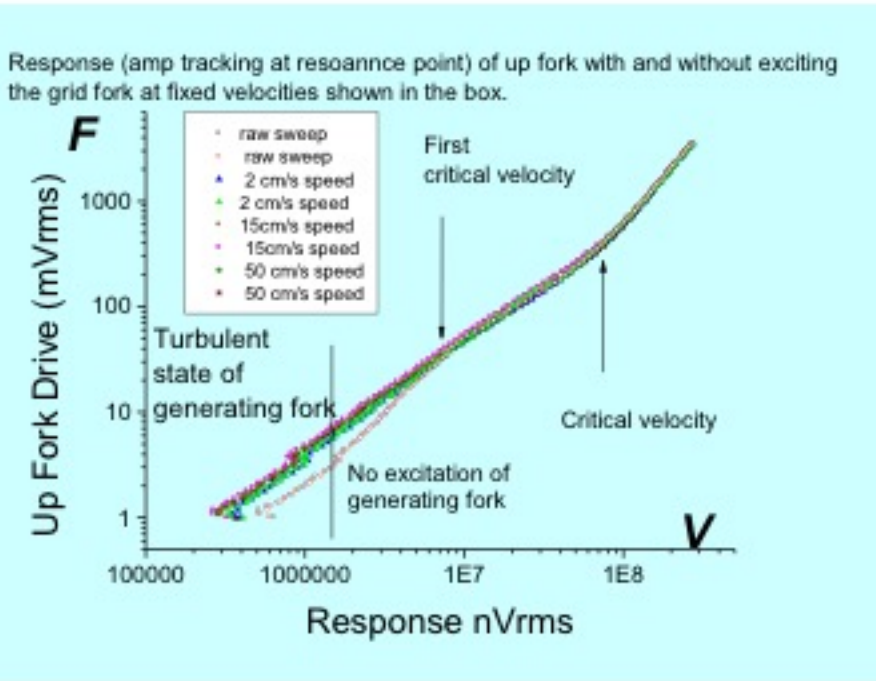

Fig 7: Influence of detecting fork response (prongs velocity) at different excitation (force of excitation and fluid resistance). The different colour corresponds to different fixed velocities of generating fork (and level of generated by this fork density of vortexes).

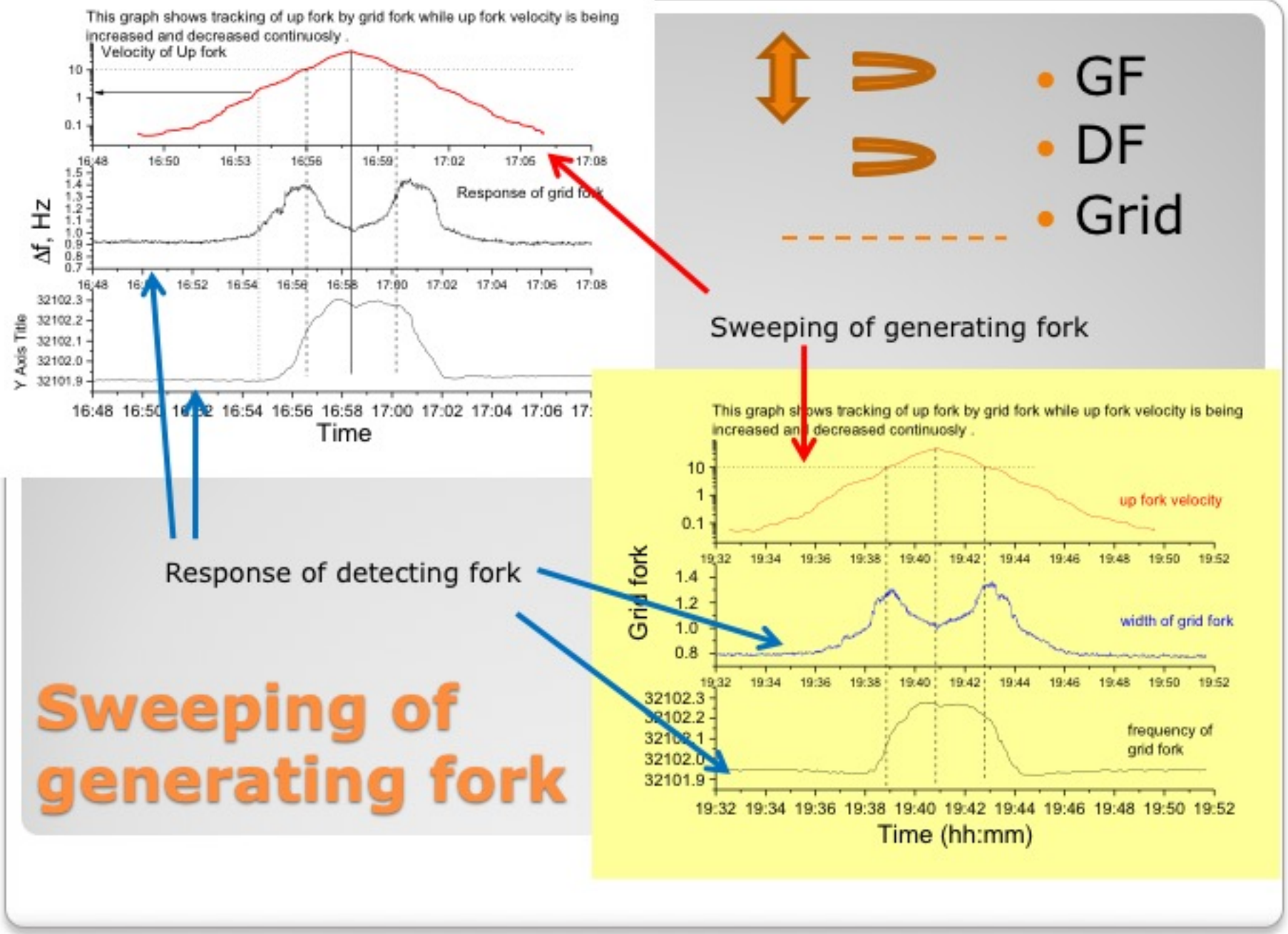
This graph shows tracking of up fork by grid fork while up fork velocity is being increased and decreased continuosly .
Velocity of Up fork
Response of grid fork
Δf, Hz
Y Axis Title
Time
GF
DF
Grid
Sweeping of generating fork
Response of detecting fork
Sweeping of generating fork
This graph shows tracking of up fork by grid fork while up fork velocity is being increased and decreased continuosly .
up fork velocity
width of grid fork
frequency of grid fork
Grid fork
Time (hh:mm)

Tuning fork behaviour at low temperatures

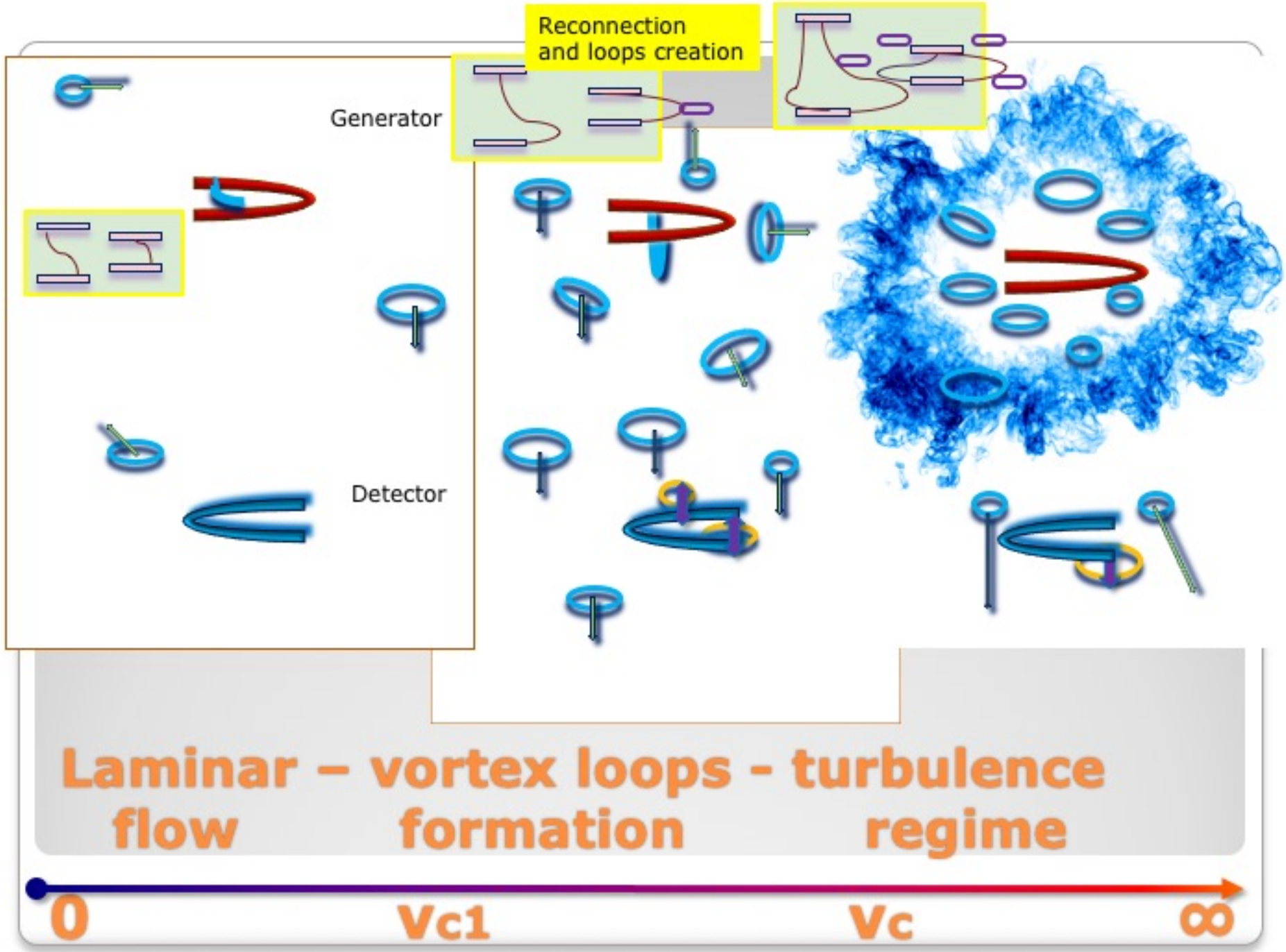
Reconnection
and loops creation
Generator
Detector
Laminar – vortex loops - turbulence
flow formation regime
0
Vc1
Vc
∞

Grid experiments

Membrane vibration

f_{R1}=765 Hz

[0,1]

$$f_{T1} = \frac{2.405}{2\pi R}\sqrt{T/\sigma}$$

f_{R1}=1756 Hz

[0,2]

$$f_{T2} = 2.296 * f_{T1}$$

[0,3]

$$f_{T2} = 3.600 * f_{T1}$$

T – surface tension, σ – area density, R – radius of membrane

At room T Δf =7.2 Hz, at base T (~10 mK) – Δf =0.004-0.006 Hz

At room T f ~765 Hz, at base T (~10 mK) – f ~ 925 Hz

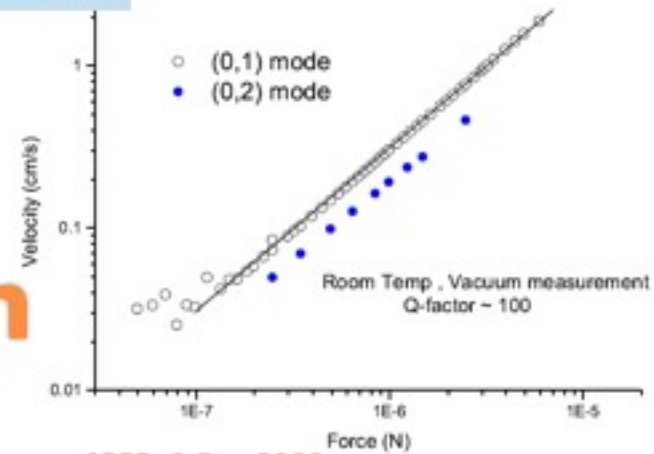

Scheme of experiments

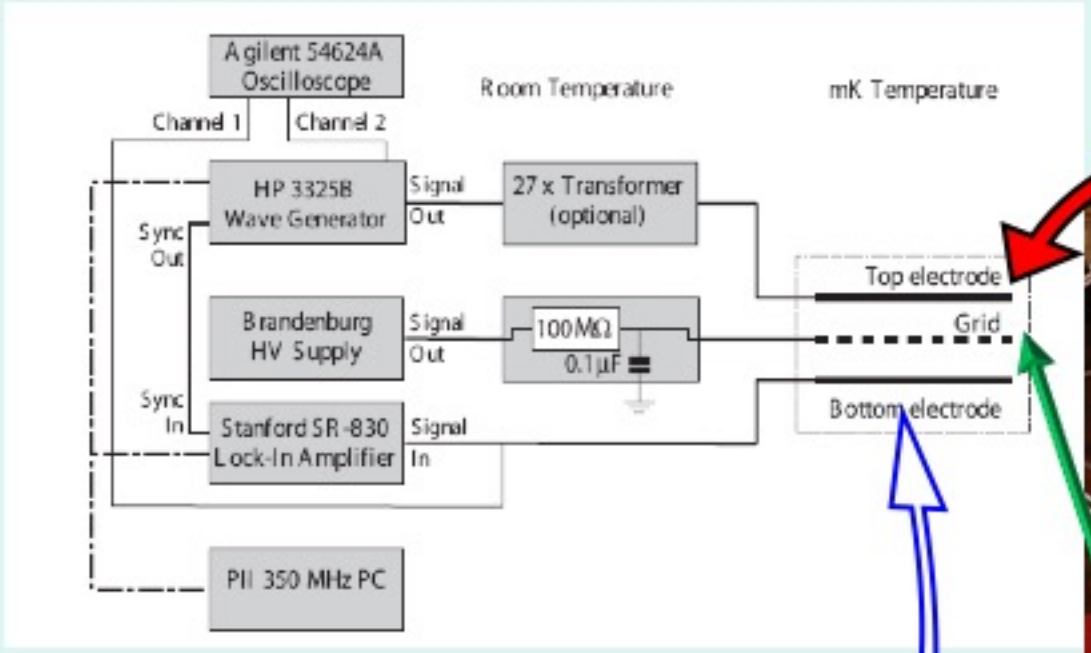

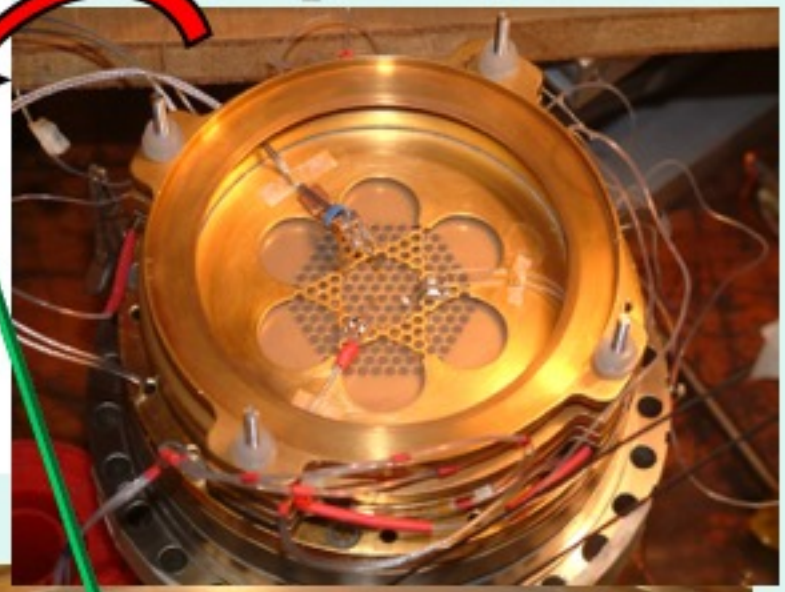

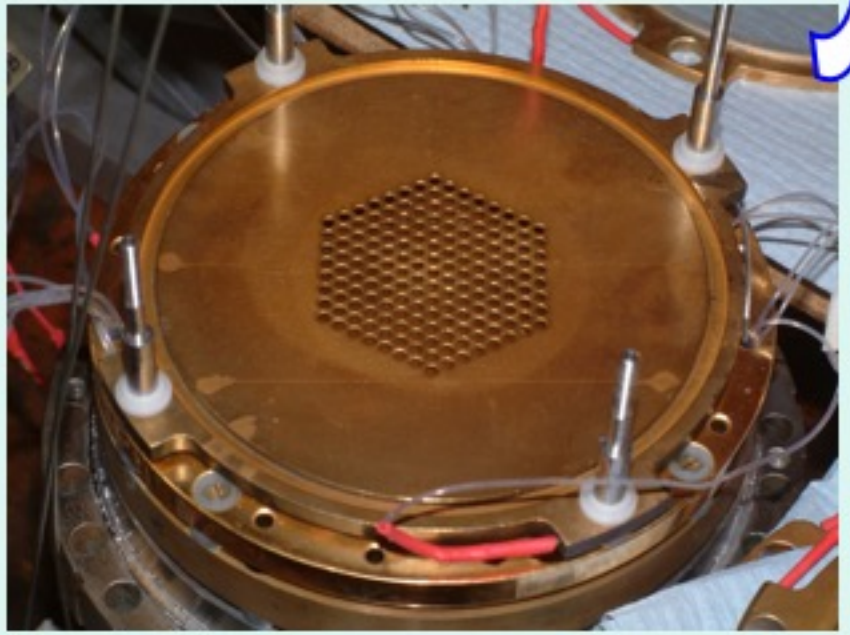

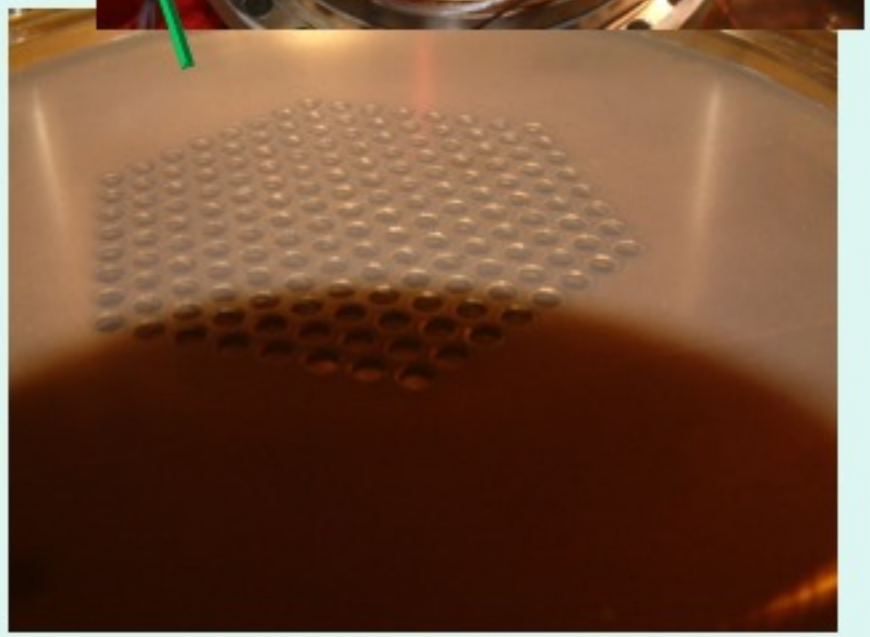

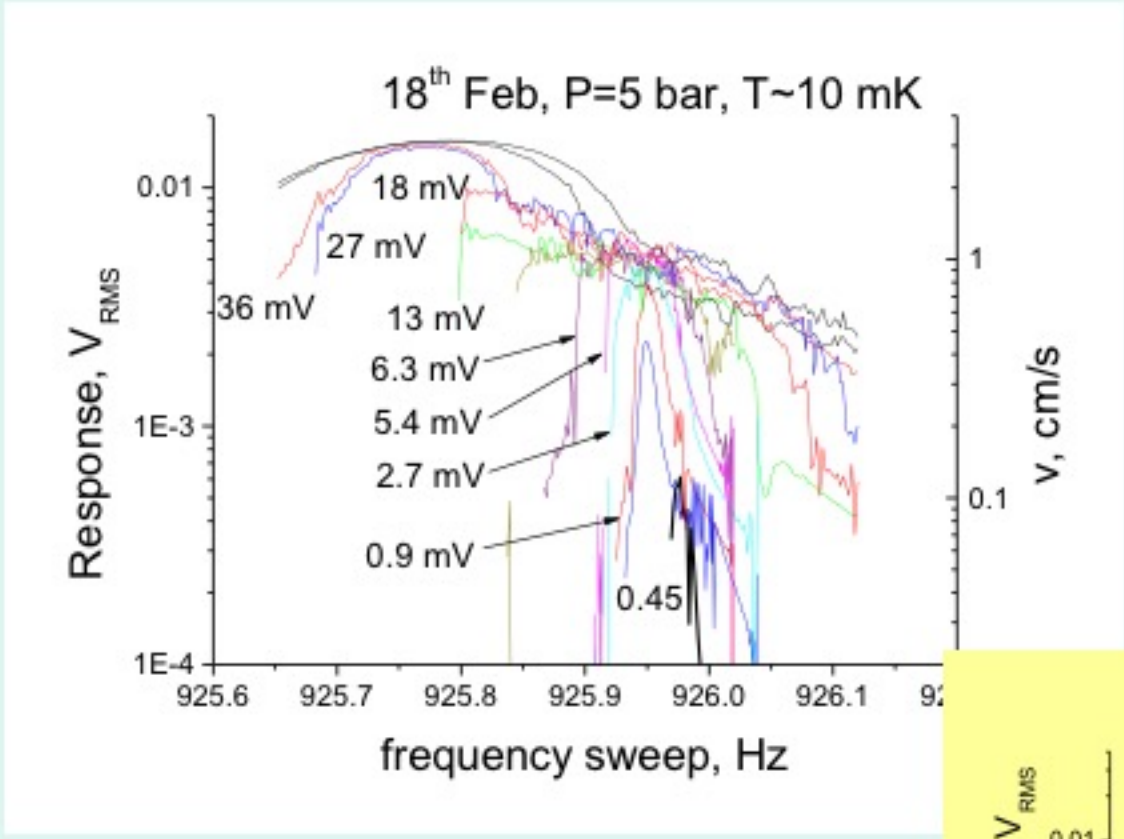
18th Feb, P=5 bar, T~10 mK
Response, V RMS
0.01
1E-3
1E-4
18 mV
27 mV
36 mV
13 mV
6.3 mV
5.4 mV
2.7 mV
0.9 mV
0.45
1
0.1
v, cm/s
925.6
925.7
925.8
925.9
926.0
926.1
frequency sweep, Hz

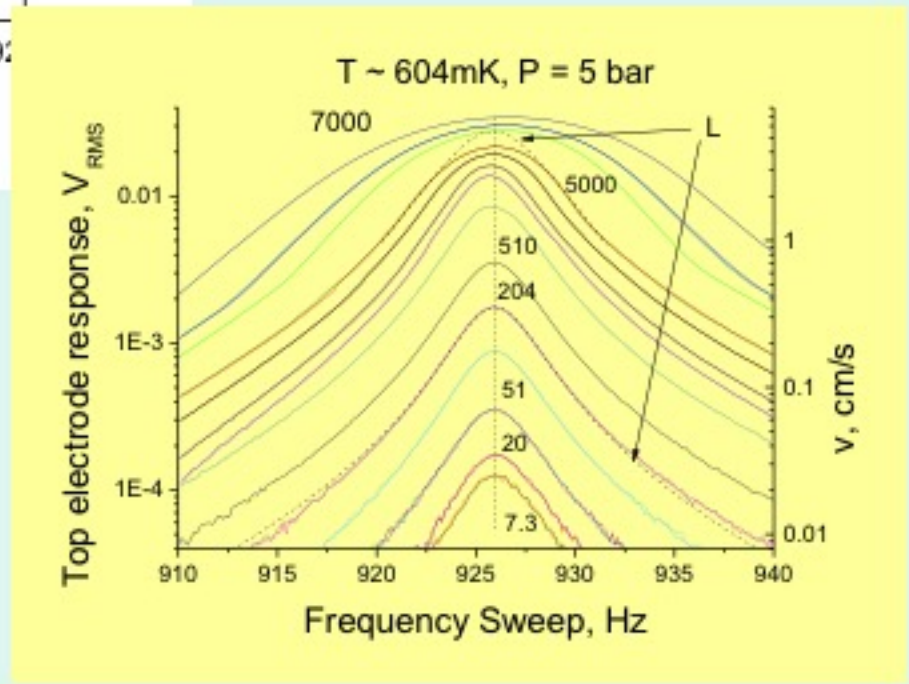
T ~ 604mK, P = 5 bar
Top electrode response, V RMS
0.01
1E-3
1E-4
7000
5000
510
204
51
20
7.3
L
1
0.1
0.01
v, cm/s
910
915
920
925
930
935
940
Frequency Sweep, Hz

Free decay of grid oscillation

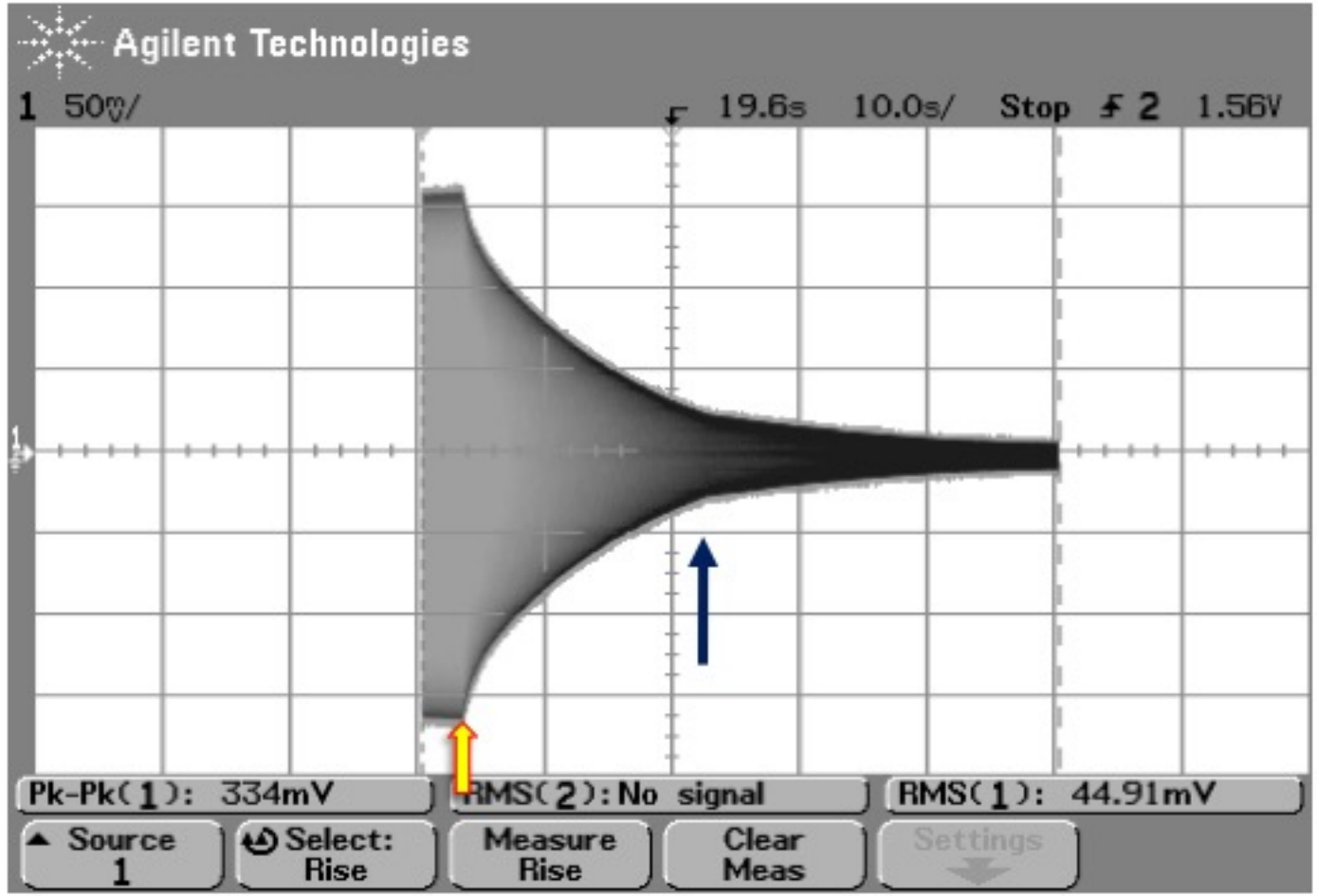

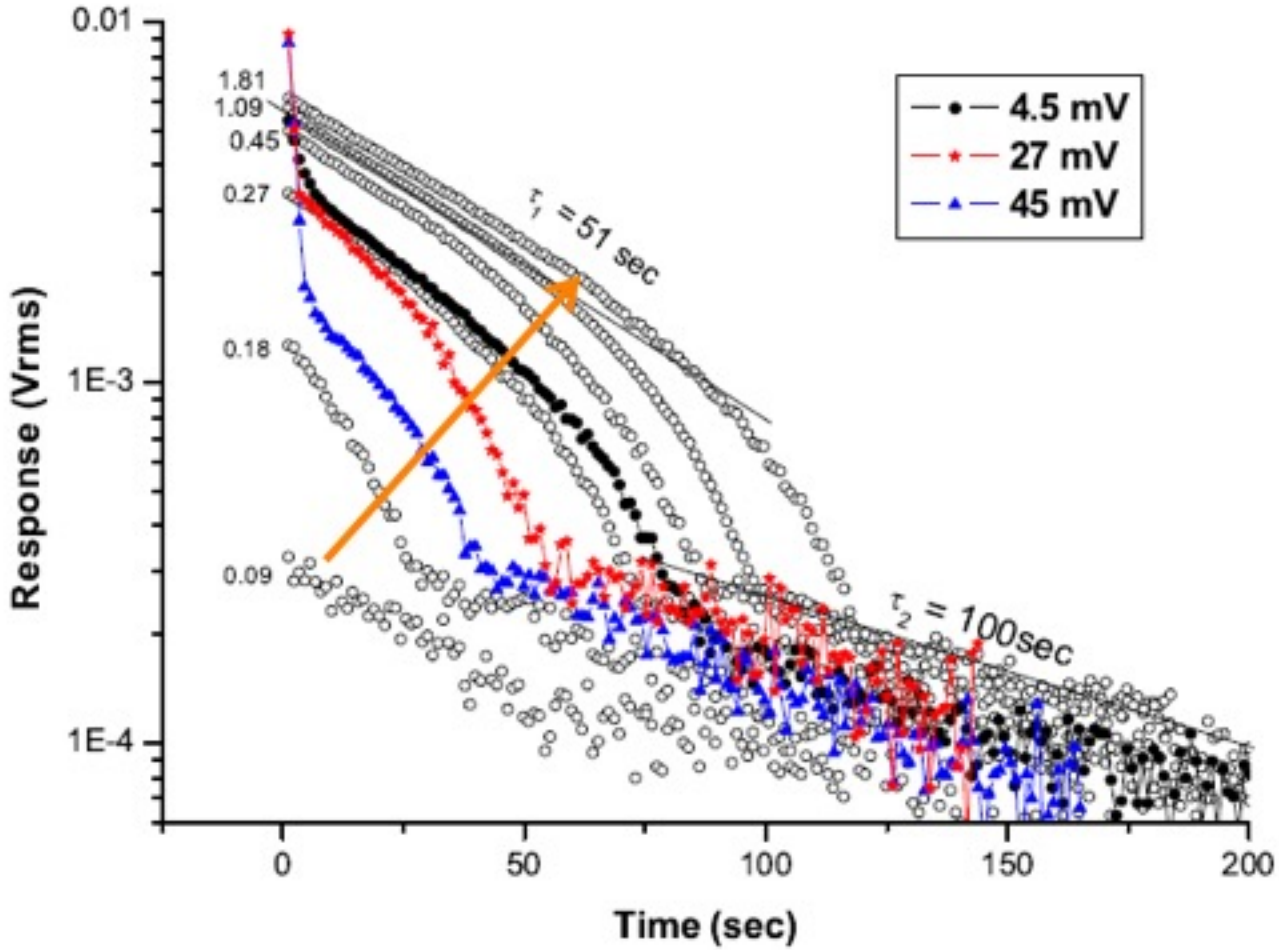

T~44 mK

Free decay of grid vibration

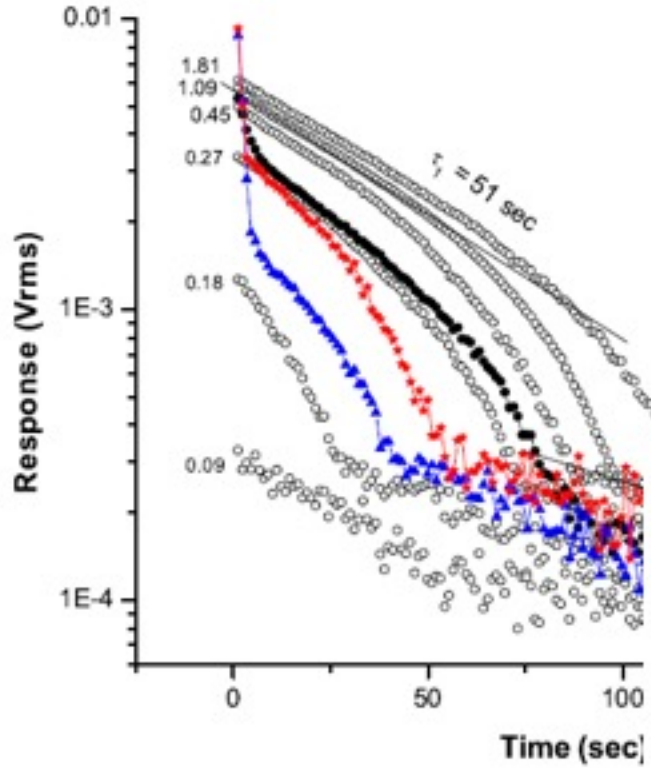
0.01
1E-3
1E-4
Response (Vrms)
1.81
1.09
0.45
0.27
0.18
0.09
τ_1 = 51 sec
0
50
100
Time (sec)

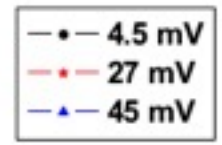
4.5 mV
27 mV
45 mV

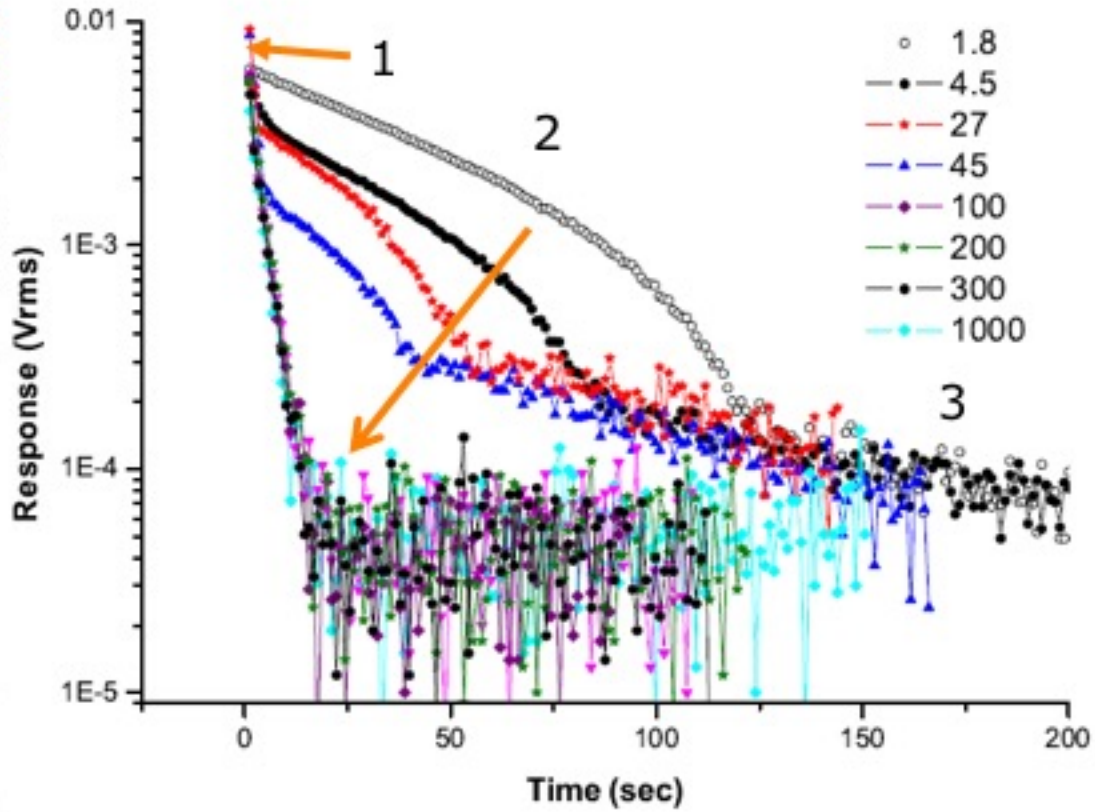
0.01
1E-3
1E-4
1E-5
Response (Vrms)
1
2
3
1.8
4.5
27
45
100
200
300
1000
0
50
100
150
200
Time (sec)

Torsion tuning forks

New tuning fork vibration modes

Flexible modes

Twisting modes

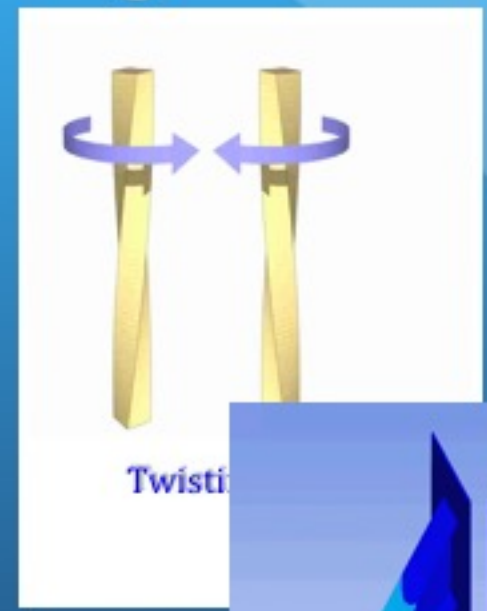

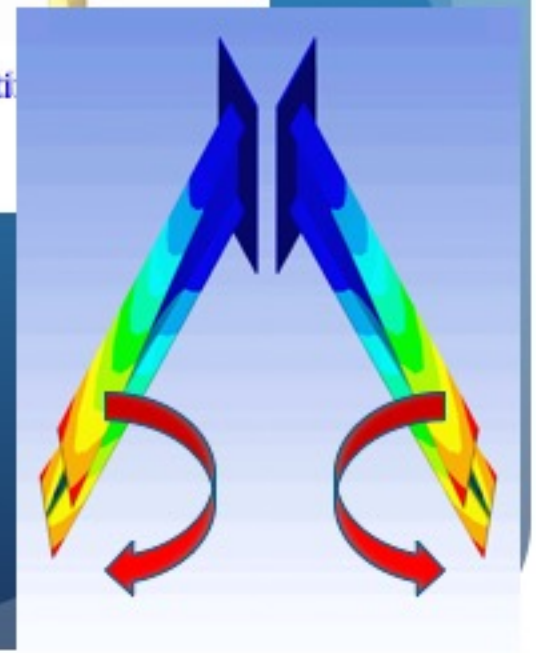

Size and vibration modes

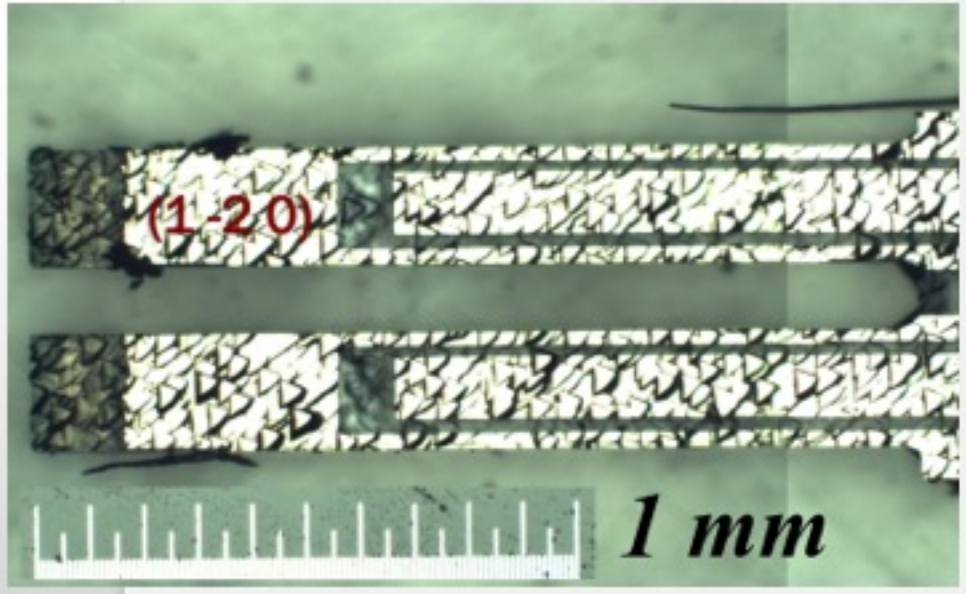

L=1.61 mm - length
T=0.223 mm - thickness
W=0.143 mm – width

Mode of vibration: bending

$$\omega_n = 2\pi f_n = \sqrt{\frac{EI}{\mu}}\frac{\beta_n^2}{L^2}$$

f_1=77.2 kHz, f_2= 482 kHz
f_3=1.35 MHz

Measured vacuum T_{room}
f_1=76,228 kHz; f_3=1.112 MHz

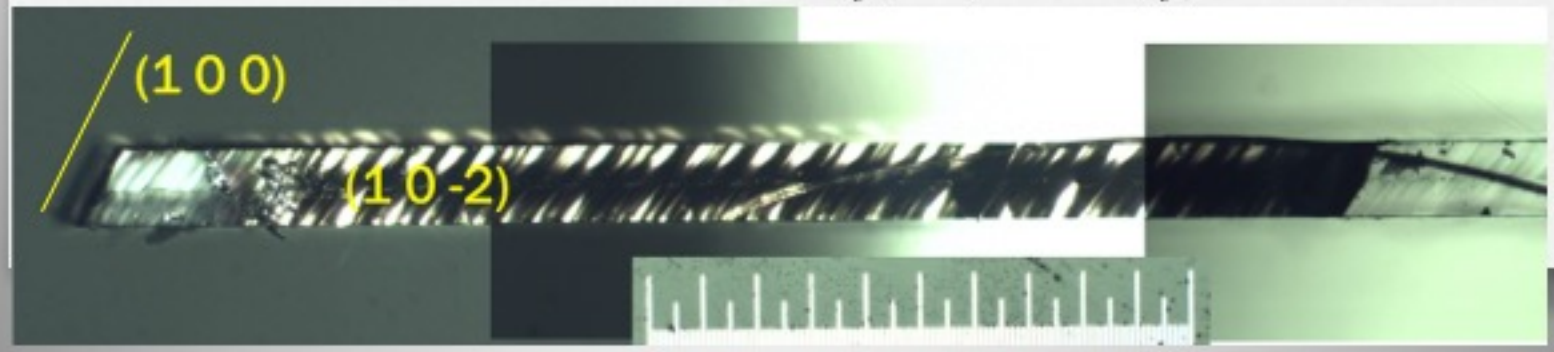

Size and vibration modes

Mode of vibration: twisting

$$G = \left(\frac{2L\omega_n}{n}\right)^2 \rho_q K$$

$$K = \frac{\left(\frac{W}{T}\right) + \left(\frac{T}{W}\right)}{4\left(\frac{W}{T}\right) - 2.52\left(\frac{W}{T}\right)^2 + 0.21\left(\frac{W}{T}\right)^6}$$

f_1=424 kHz, f_2= 848 kHz
f_3=1272 kHz

Measured vacuum T_{room}
f_1=393 020 Hz

$f_B \sim f_1 * (2n-1)$
$f_T \sim f_1 * n$

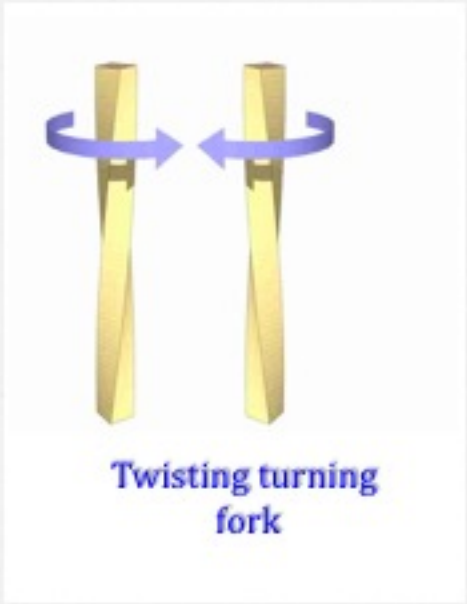

Twisting turning fork

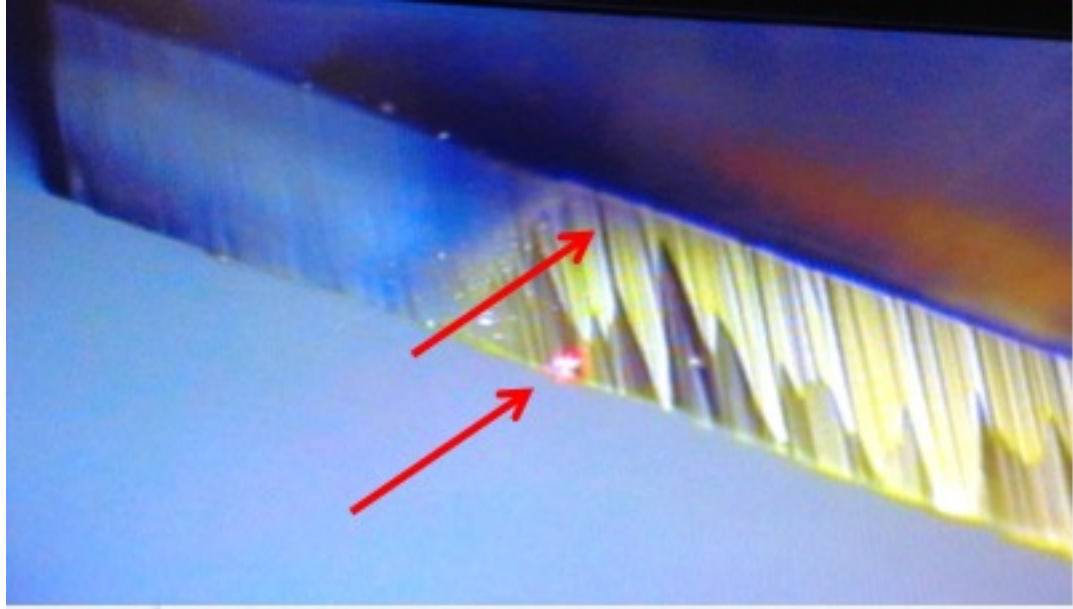

f = 393 093 Hz, Δf=60 Hz;
velocity of vibration v_P=10.4 cm/s

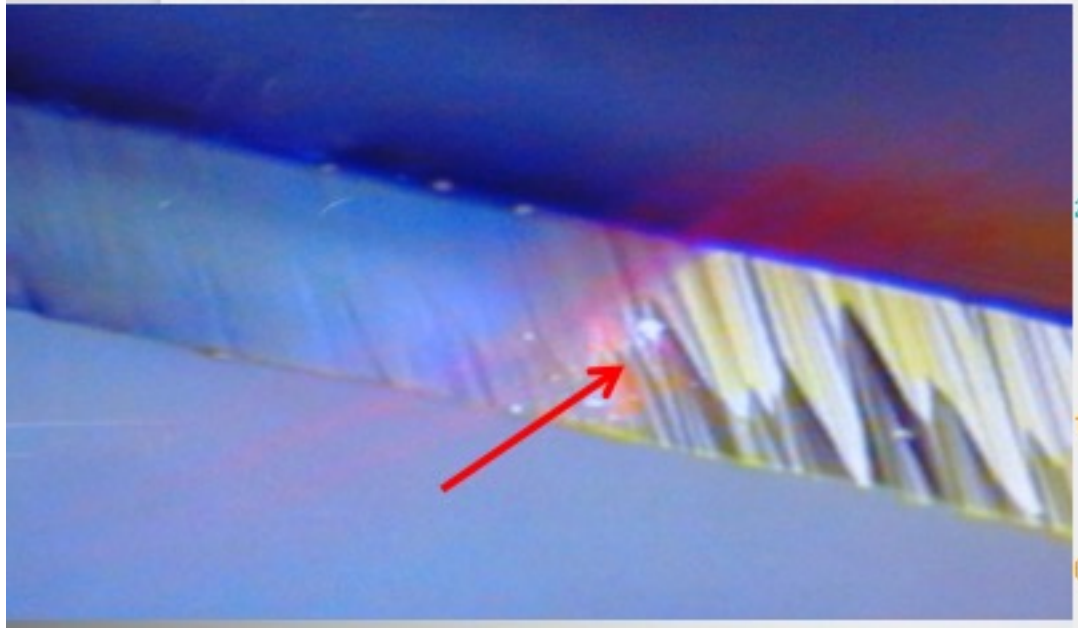

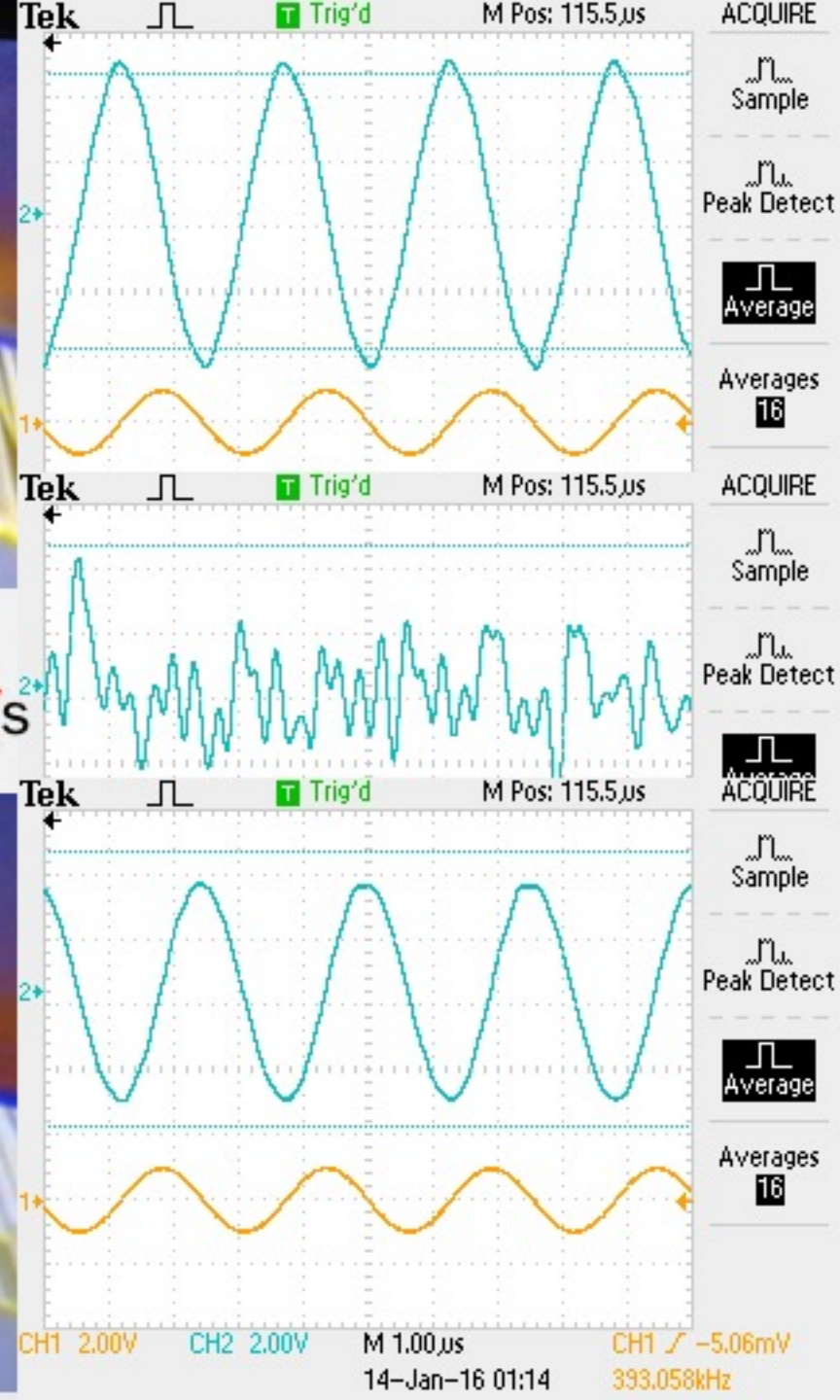

Torsion fork motion at different modes

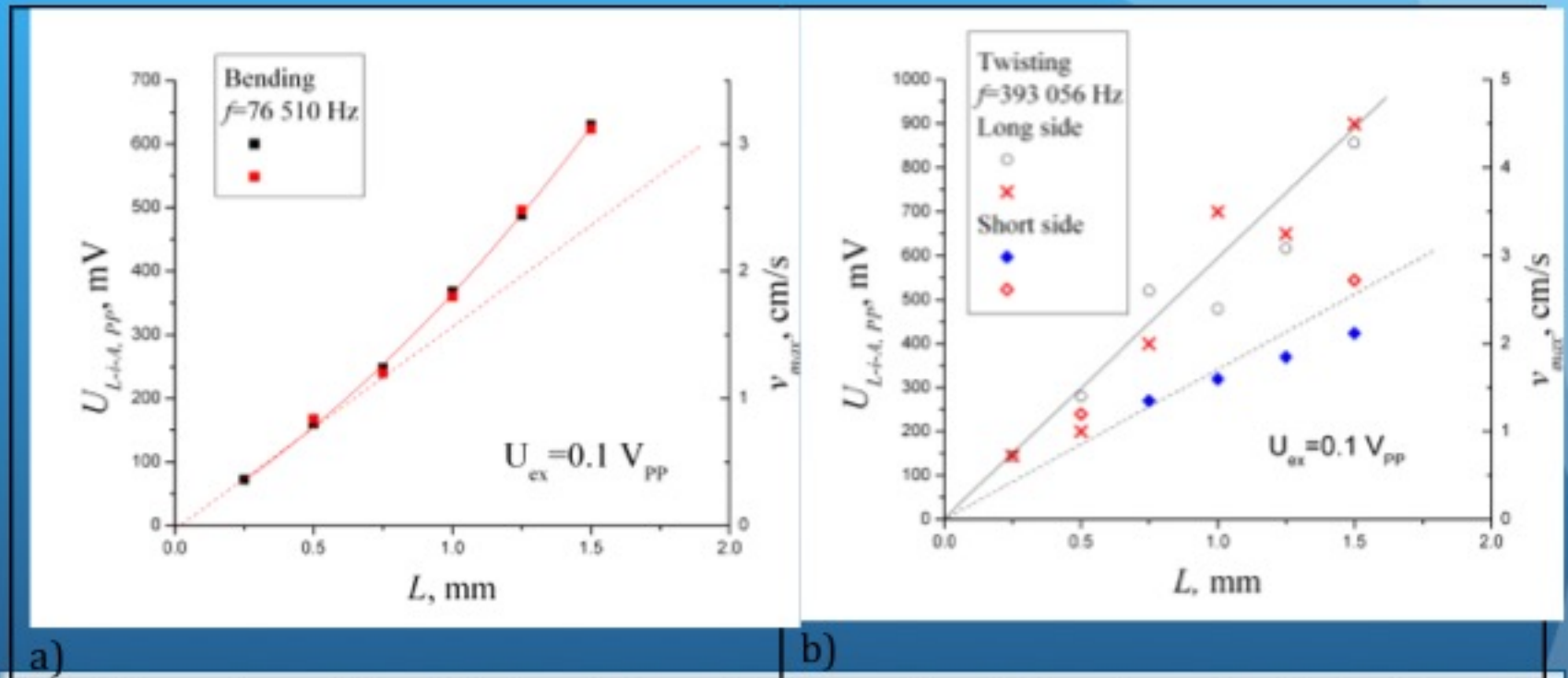

a) b)

Fig.3 Scanning of the DA signal along the prong for different mode of vibration, a) bending mode and b) twisting mode from different sides of the prong. The right scale indicates a prong velocity (results 2017, air, T_{room}).

Different media of fork vibrations

Calibration of I-V convertor.

393 kHz 0.571 V on R=33 kOm Uex=0 dB

76 kHz 0.629 V on R=33 kOm Uex=0 dB

Frequency of resonance U_{ex}=0dB (1V):

Gases	Vacuum Room	He Room Air	Room	N2 Low T
393kHz	393 020,1	393 014,75	392 973,5	392 653.5
76 kHz	75 663,24	75 688,8	75 643,75	75 927,6

Liquids	SF He T=1.4 K	He T=4.2 K	Liquid N_2	N2 Low T
393kHz	387 892,5	388 372,5	371 997,5	392 653.5
76 kHz	74 308,9	74 458	67 567,5	75 927,6

Different media of fork vibrations

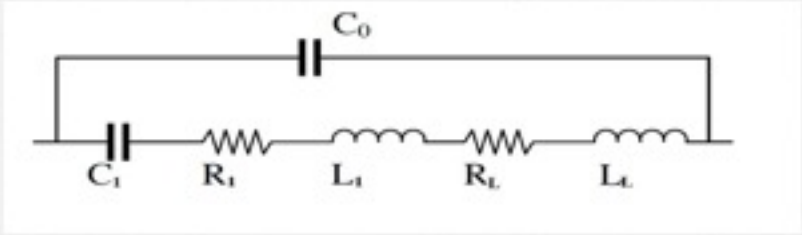

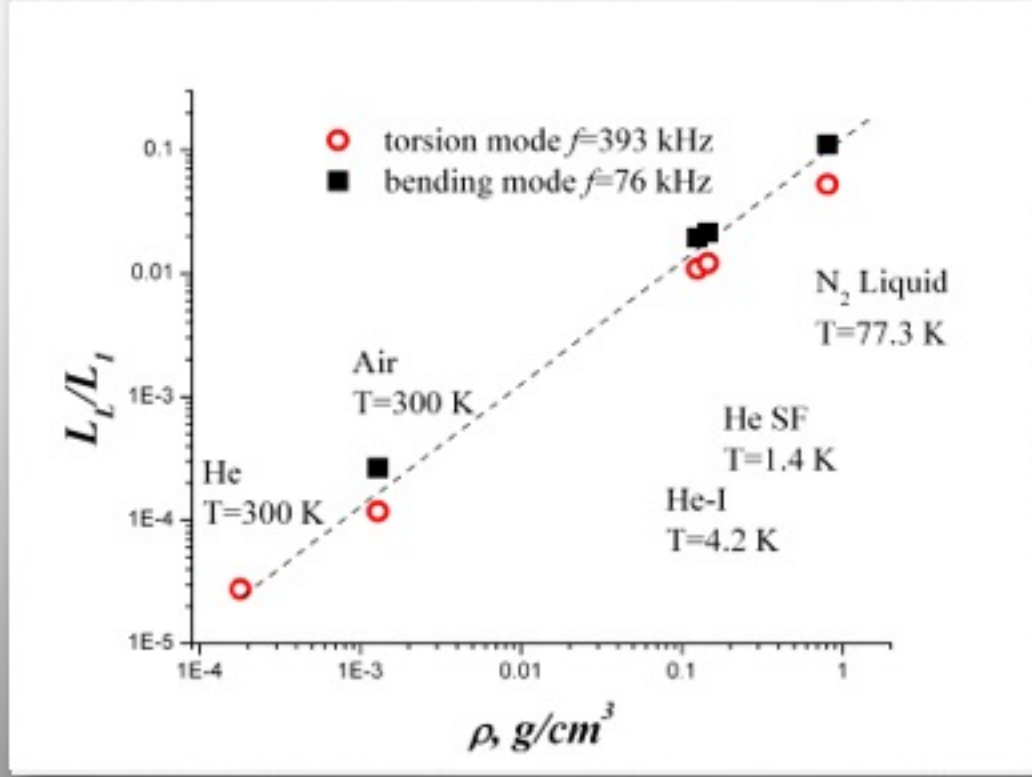

The resonant frequency of the circuit is given by

$$f = \frac{1}{2\pi\sqrt{(L_1 + L_L) * C_1}}$$

The resonant frequencies were measured in different media, so for these measurements changed only L_L

$$\Delta f \cong -\frac{1}{2} f_1 \frac{L_L}{L_{1:}}$$

Fork vibration in superfluid helium

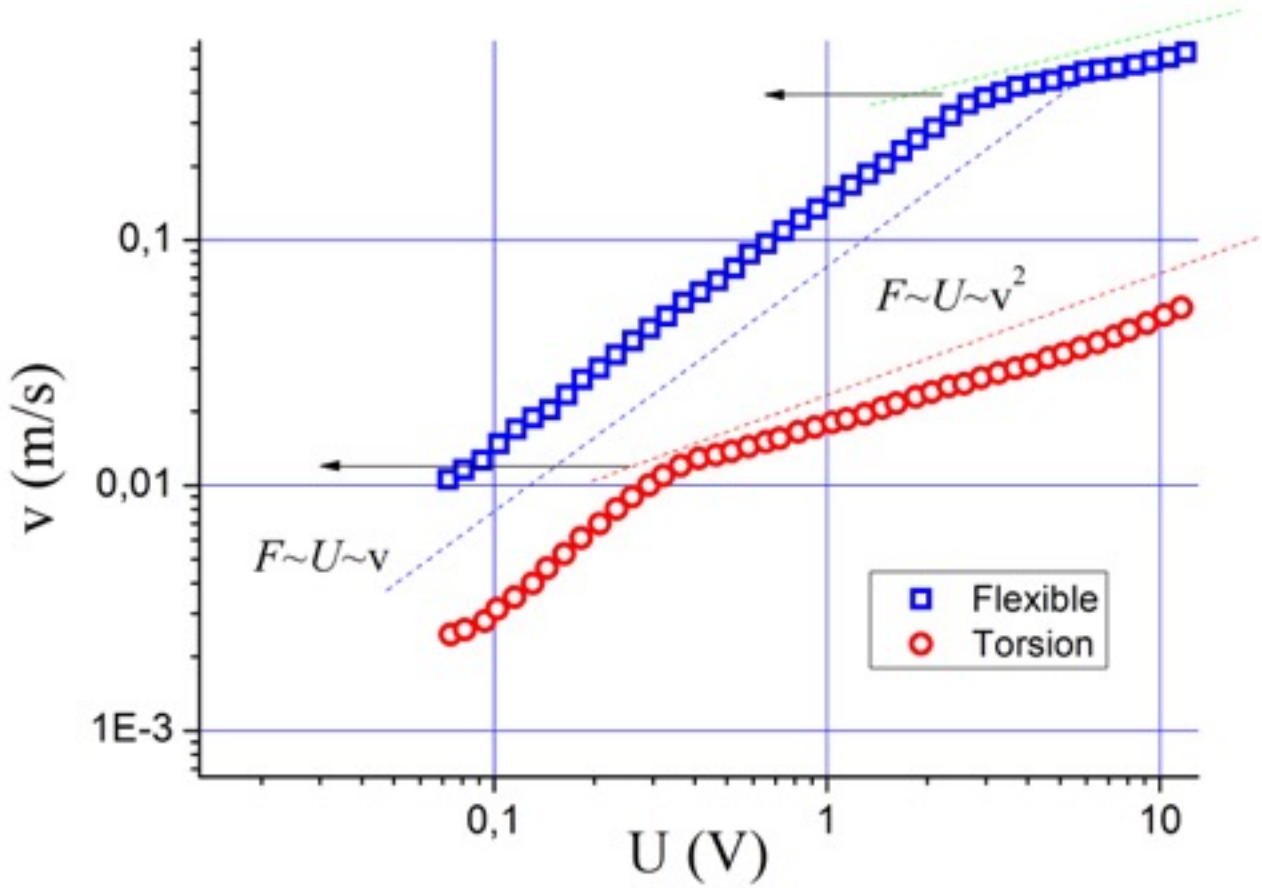

Conclusions

- Tuning forks are cheap, robust, reproducible, easy to install and very sensitive;
- Vibrating forks in superfluid helium use as a generator and a detector of turbulence;
- Influence of one fork on another at distance more bigger the size of fork – the vertexes move through cm's distance at T~0 K;
- Virgin and disturb states exist in superfluid helium. The disturb state maintains hundreds hours at base temperatures (T~10 mK);
- The energy loss of vibrating grid at free decay and tuning forks comes through three stages:

  - very quick energy loss – energy pumping into turbulent state (inject of vortex loop flux or classical turbulence?),
  - quick linear loos of energy (create of vortexes?),
  - slow free vibration (laminar motion, quality of grid);
- The torsion tuning fork has two modes: flexible and twisting. The transition into turbulent state has drastically different critical velocities for bending and twisting motion.